

Development of a High Latent Effectiveness Energy Recovery Ventilator with Integration into Rooftop Package Equipment

Final Report

Reporting Period Start: October 1, 2001

Reporting Period End: December 31, 2005

**Principal Authors: Gregory M. Dobbs, Norberto O. Lemcoff,
Frederick J. Cogswell, and
Jeffrey T. Benoit**

March 2006

DOE Cooperative Agreement DE-FC26-01NT41254

UTRC Report R2006-6.400.0005-F-FR01

Prepared by:

**United Technologies Research Center
411 Silver Lane
East Hartford, CT 06108
Gregory M. Dobbs, Principal Investigator**

Prepared for:

**U.S. Department of Energy
National Energy Technology Laboratory
3610 Collins Ferry Road
Morgantown, WV 26505
P. Steven Cooke, Program Manager**

Subcontractors:

**Center for Automation Technologies
Suite CII8015
Rensselaer Polytechnic Institute
Troy, NY 12180**

**Center for Building Performance & Diagnostics
Department of Architecture
Carnegie Mellon University
5000 Forbes Avenue
Pittsburgh, PA 15213-3890**



Research Center

Disclaimer

This report was prepared as an account of work sponsored by an agency of the United States Government. Neither the United States Government nor any agency thereof, nor any of their employees, makes any warranty, express or implied, or assumes any legal liability or responsibility for the accuracy, completeness, or usefulness of any information, apparatus, product, or process disclosed, or represents that its use would not infringe privately owned rights. Reference herein to any specific commercial product, process, or service by trade name, trademark, manufacturer, or otherwise does not necessarily constitute or imply its endorsement, recommendation, or favoring by the United States government or any agency thereof. The views and opinions of authors expressed herein do not necessarily state or reflect those of the United States Government or any agency thereof.

Acknowledgements

The Principal Investigator for this project, Dr. Gregory M. Dobbs, would like to acknowledge the technical contributions and reporting of UTRC staff that were responsible for specific activities. Dr. Mary Saroka was responsible for the intrinsic moisture transfer properties of membrane materials and the aerodynamic and heat transfer testing of pieces of lattice block separator material. Allen Murray and Robert Hebert provided valuable experimental technical assistance. Dr. Frederick J. Cogswell was responsible for creating the preliminary design for a rooftop-integrated device, and directed the experimental program including facility testing and controls development. He was ably assisted in the laboratory by James A. Davies, Heidi Hollick, Christopher Chipman and Salvatore Saitta. Dr. Jeffrey Benoit carried out studies on reliability. Dr. Norberto Lemcoff functioned as a Program Manager and interface to Carrier personnel and directed some of the experimental work. Glenn Saunders and Prof. Daniel Walczyk, who led the subcontractor effort at RPI, not only performed the RPI Statement of Work, but also contributed as integrated members of the team. Profs. Stephen R. Lee and Khee Poh Lam led the modeling effort at Carnegie Mellon University assisted by Chaoquin Zhai and Yi Chun Huang.

Abstract

This Final Report covers the Cooperative Program carried out to design and optimize an enhanced flat-plate energy recovery ventilator and integrate it into a packaged unitary (rooftop) air conditioning unit. The project objective was to optimize the design of a flat-plate energy recovery ventilator (ERV) core that compares favorably to flat plate air-to-air heat exchanger cores on the market and to cost wise to small enthalpy wheel devices. The benefits of an integrated unit incorporating an enhanced ERV core and a downsized heating/cooling unit were characterized and the design of an integrated unit considering performance and cost was optimized.

Phase I was to develop and optimize the design of a membrane based heat exchanger core. Phase II was the creation and observation of a system integrated demonstrator unit consisting of the Enhanced Energy Recovery Ventilator (EERV) developed in Phase I coupled to a standard Carrier 50HJ rooftop packaged unitary air conditioning unit. Phase III was the optimization of the system prior to commercialization based on the knowledge gained in Phase II. To assure that the designs chosen have the possibility of meeting cost objectives, a preliminary manufacturability and production cost study was performed by the Center for Automation Technologies at RPI. Phase I also included a preliminary design for the integrated unit to be further developed in Phase II. This was to assure that the physical design of the heat exchanger designed in Phase I would be acceptable for use in Phase II. An extensive modeling program was performed by the Center for Building Performance & Diagnostics of CMU. Using EnergyPlus as the software, a typical office building with multiple system configurations in multiple climatic zones in the US was simulated. The performance of energy recovery technologies in packaged rooftop HVAC equipment was evaluated. The experimental program carried out in Phases II and III consisted of fabricating and testing a demonstrator unit using Carrier Comfort Network (CCN) based controls. Augmenting the control signals, CCN was also used to monitor and record additional performance data that supported modeling and conceptual understanding. The result of the testing showed that the EERV core developed in Phase I recovered energy in the demonstrator unit at the expected levels based on projections. In fact, at near-ARI conditions the core recovered about one ton of cooling enthalpy when operating with a three-ton rooftop packaged unit.

Development of a High Latent Effectiveness energy Recovery Ventilator with Integration into Rooftop Package Equipment:

Final Report

Table of Contents

Abstract.....	iii
1.0. Executive Summary	1
2.0 Introduction.....	3
2.1. Experimental	5
3.0 Membrane Core Optimization	6
4.0 Preliminary EERV/Rooftop Integrated Design	11
5.0 Manufacturability Study	13
6.0 Modeling the Performance of Integrated EERV/Rooftop Equipment.....	18
7.0 Integrated Packaged Unitary EERV-Rooftop Demonstrator.....	24
8.0 Results and Discussion	61
8.1 EERV Reliability Analysis	61
9.0 Commercialization Plan.....	66
10.0 Conclusions.....	67
11.0 Principal Project Personnel.....	69
12.0 References.....	70
13.0 List of Acronyms and Abbreviations.....	71

List of Figures

Figure 2.1. Airstream numbering conventions.	3
Figure 2.2. Effectiveness factors of current devices.....	4
Figure 2.3. Comparison of membrane and paper core effectiveness as a function of size.....	4
Figure 3.1. Lattice block structure. The orientation on the left is the “high-stirring/high pressure drop orientation”. The view on the right is the “lower-pressure drop/lower-stirring” orientation.	7
Figure 3.2. (a) Demonstration small piece of lattice block structure at program inception. Blue dye was added to the plastic to increase visibility.....	8
Figure 3.3. Photograph of the alternative mesh spacer.....	9
Figure 4.1. Consumed energy with and without EERV for three cities.	12
Figure 4.2. Energy usage with and without EERV for three cities normalized to the no EERV case.	12
Figure 5.1. Alternative design comparison: membrane utilization with respect to total EERV volume.	14
Figure 5.2. Alternative design comparison: membrane utilization with respect to active EERV volume	14
Figure 6.1. National map of annual energy savings by location with an enhanced energy recovery ventilator with a packaged unitary HVAC unit using a fixed downsizing.	22
Figure 6.2. Interpolated representation of the same data displayed in Figure 6.1.	23
Figure 7.1. Rooftop schematic of EERV/rooftop integrated system.	24

Figure 7.2. EERV core assembly for demonstrator unit.	25
Figure 7.3. Test facility schematic.	26
Figure 7.4. View of test hardware in outdoor chamber.	28
Figure 7.5. Additional facility views.	29
Figure 7.6. Facility control modes.	31
Figure 7.7. EERV test facility at UTRC.	32
Figure 7.8. Carrier performance curves for 50HJ running at 1200 cfm.	33
Figure 7.9. Psychrometric chart during a validation run.	35
Figure 7.10. Normal operating conditions of integrated system.	36
Figure 7.11. Mixing conditions in EERV mode and non-EERV mode.	38
Figure 7.12. Operation with humid outdoor conditions.	40
Figure 7.13. Operation with humid indoor and outdoor conditions.	40
Figure 7.14. Psychrometric chart with stream conditions identified for a. cool and damp outside air run	41
Figure 7.15. Transients during high-flow run.	43
Figure 7.16. Psychrometric paths with and without an ERV preprocessor.	45
Figure 7.17. Optimized integrated EERV/Rooftop unit. Front view on return and mixing-box side with fresh air flow (blue) visible into mixing box.	46
Figure 7.18. EERV core in custom Plexiglas® manifold. Protective paper has not yet been removed.	47
Figure 7.19. Close up view of the horizontally-oriented EERV core attached across the top of the rooftop.	47
Figure 7.20. View of the completed integrated EERV/rooftop unit.	48
Figure 7.21. Schematic of new configuration showing fan locations and flow measurement stations.	49
Figure 7.22. Exhaust fan performance and core pressure drop.	50
Figure 7.23. Economizer positioned for installation into the rooftop unit.	51
Figure 7.24. Total enthalpy load and fan power shown for a) 300 W fan power at 400 cfm, and b) 150 W fan power at 400 cfm.	53
Figure 7.25. Experimental set up with leak paths shown.	56
Figure 7.26. 50% mixing after recovery.	56
Figure 7.27. Schematic of just core assembly showing leakage paths.	57
Figure 7.28. Third in a series of CO ₂ leak tests. This test was done after the box was opened and potential leak paths within the box itself were sealed with clay and metallic tape. At time zero CO ₂ was flowed into plenum (1), and measurements began in plenum (2). At 90 seconds into the test the CO ₂ probe was moved to plenum (4).	59
Figure 7.29. Same run as Figure 7.28 above, but the baseline voltage has been subtracted from each of the two lines to remove the effect of the rising background.	59
Figure 7.30. Final CO ₂ leak test. Same condition as previous test except that the exhaust fan was run at a higher speed.	60

List of Tables

Table 3.1	Tested Membrane Summary	6
Table 3.2	Performance Goals and Results	10
Table 5.1	Cost Breakdown at 40,000 EERV's Per Year.....	16
Table 5.2	Implications of Design Change on Projected Manufacturing Cost	17
Table 7.1.	Integrated System Airflows	25
Table 7.2.	List of Measurement Stations	26
Table 7.3.	List of Facility and Test Unit Actuators	27
Table 7.4.	Carrier Performance Tables for UTRC's EERV Facility Rooftop	34
Table 7.5	Sample of Data Collected in EERV Mode	35
Table 7.6	Sample of Data Collected in Non-EERV Mode	36
Table 7.7	EERV Actuators	37
Table 7.8	Sample Fan Power Calculation.....	39
Table 7.9	Low Sensible /High Humidity Load Run	41
Table 7.10	Reproducibility Run Results.....	42
Table 7.11	High Face Velocity Run	42
Table 8.1	EERV Reliability Requirements	61

1.0. Executive Summary

This Final Report covers the Cooperative Program carried out to design and optimize an enhanced flat-plate energy recovery ventilator and integrate it into a packaged unitary (rooftop) air conditioning unit. The project was divided into three Phases. Phase I was to develop and optimize the design of a membrane based heat exchanger core. To assure that the designs chosen have the possibility of meeting cost objectives, a preliminary manufacturability and production cost study was performed by the Center for Automation Technologies at RPI. A detailed design for a counter-flow, Enhanced Energy Recovery Ventilator (EERV) utilizing a proprietary membrane to efficiently transfer sensible and latent heat between air streams, for use in rooftop air handling systems, was carried out. Estimates for the cost of the components making up the EERV were developed, and manufacturing systems to produce it were conceptualized. This information and the concepts are used to develop estimates for the manufacturing costs associated with producing the EERV at differing annual production rates. The manufacturing cost of an EERV of comparable size to existing non-membrane based Energy Recovery Ventilators currently on the market, at an annual production volume of 40,000 units and using fully automated assembly systems, is estimated to be approximately \$200. Phase I also included a preliminary design for the integrated unit to be further developed in Phase II.

Phase II was the creation and observation of a system integrated demonstrator unit consisting of the Enhanced Energy Recovery Ventilator (EERV) developed in Phase I coupled to a standard Carrier 50HJ rooftop packaged unitary air conditioning unit. This was to assure that the physical design of the heat exchanger designed in Phase I would be acceptable for use in Phase II.

An extensive modeling program was performed and EnergyPlus was selected as the software platform that was most likely to give the required fidelity. The program consisted in the creation of 16 EnergyPlus input files that reflected a standard office building equipped with one of four sizes of cooling plant and which could have an economizer, an EERV both or neither, and a geographical survey in which results were obtained on the value of energy recovery for 62 U.S. cities. Test models were developed for simulation runs on five HVAC system configurations with weather data from Miami, Florida, and then simulations were run for different climatic conditions to provide additional comparisons of system performance. The HVAC system configurations were based upon both CAV and CAV+ERV with and without economizer cycles and CAV+ERV with bypass control. Results show the effect of DX coil capacity on energy consumption and on meeting indoor design conditions for temperature and relative humidity. The data illustrates that as DX coil capacity is increased, energy consumption increases, indoor temperature control increases and indoor relative humidity control decreases.

The simulated results obtained in this study for this building type, building occupancy and system configuration fall comfortably within the range of accepted rules of thumb within the HVAC industry for system sizing and annual energy conditions. Empirical testing under controlled conditions would be required to further validate the EnergyPlus model.

The experimental program consisted of fabricating and testing the demonstrator unit using Carrier Comfort Network (CCN) based controls. Augmenting the control signals, CCN was also used to monitor and record additional performance data that supported modeling and conceptual understanding. The result of the testing showed that the EERV core developed in Phase I recovered energy in the demonstrator unit at the expected levels based on projections. In fact, at

near-ARI conditions the core recovered about one ton of cooling enthalpy when operating with a three-ton rooftop packaged unit.

Phase III was the optimization of the system prior to commercialization based on the knowledge gained in Phase II. During this phase the design of the integrated unit was reworked, a control system was developed, tests of the facility were carried out, and the results analyzed to assess the implications for further product development.

The reliability of the EERV system, as well as the enthalpy wheel system, were analyzed and compared to preliminary system reliability requirements. The expected value of reliability predicted for the EERV system met the target requirement, while that of the enthalpy wheel system did not. In addition, a detailed FMEA was conducted on the both of these systems. Again the enthalpy wheel system was shown to have more risks than the EERV system, with the exception of the membranes themselves, which need additional work to become mature. A detailed reliability test plan was developed for the EERV membranes that can guide efforts to better understand and quantify the membrane risks versus possible environmental contaminants. The results of executing this test plan and analysis would serve to refine the reliability prediction for the EERV and could also inform planned maintenance schedules, control algorithms and warranty cost models.

2.0 Introduction

Enthalpy/Energy Recovery Ventilators (ERV) devices precondition the outside air entering buildings by using the already conditioned exhaust air leaving the building. Increased use of such devices has energy savings benefits for the nation and such devices can have financial advantages for the end user. While several states require the use of such devices to ventilate tight buildings it is the objective of this program to make such devices at a sufficiently low manufacturing cost that their use will become more widespread based on their economic viability rather than by regulatory requirement.

There are several market opportunities: (a) standalone units for residences that are mechanically ventilated, (b) standalone units for light commercial buildings, and (c) as a preconditioner used in direct association with HVAC equipment. For each of these segments there are specific requirements and preferences that will favor one kind of energy recovery or preconditioning technology over another in a fragmented HVAC industry.

There are many approaches for air-to-air technology. The technologies closest to the one being matured in this program will be discussed below. All of them can be discussed in terms defined by ASHRAE according to the schematic in Figure 2.1, where X_n is the dry bulb temperature, the absolute humidity ratio, or the enthalpy of airstream n . W_n is the mass flow of airstream n . ϵ is the “effectiveness factor” for temperature, humidity, or enthalpy, depending on the choice for X , respectively. The leaving supply air condition is

$$X_2 = X_1 + \epsilon \cdot (W_{\min} / W_s) (X_3 - X_1)$$

and the leaving exhaust air condition is:

$$X_4 = X_3 - \epsilon \cdot (W_{\min} / W_e) (X_1 - X_3)$$

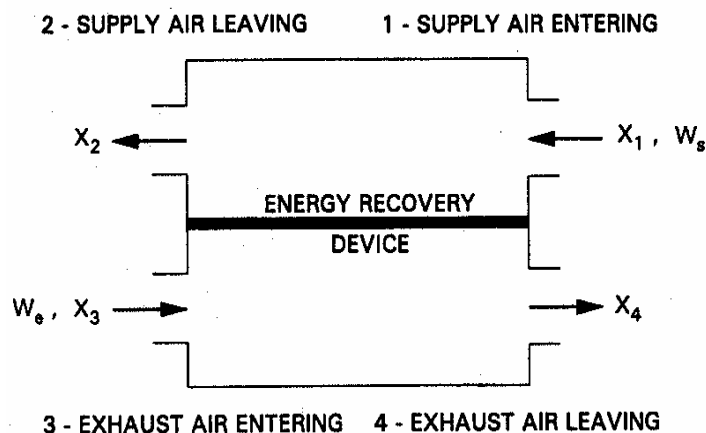


Figure 2.1. Airstream numbering conventions.

The “membrane core” or Enhanced Energy Recovery Ventilator (EERV) is a new type of air-to-air heat exchanger being developed under this program at UTRC and for which Carrier patents have now been issued. The “membrane” is a sulfonated ionomer capable of passing water vapor efficiently, but blocking the transmission of other air components across its surface. Of particular note is that *the latent performance of this configuration implies a latent heat effectiveness that is at least two or three times that of the typical paper units in the marketplace.* Figure 2.2 shows the

effectiveness values for the paper units currently sold and the goal effectiveness for the heat exchanger to result from the program. Also included for comparison is the effectiveness of a mechanical heat pump product currently sold by Carrier that is called an “Energy Recycler”. Figure 2.3 shows some prior experimental and simulation results which show how the effectiveness scales with the amount of active surface. Hence, size and materials cost are important factors in designing a device to reach a target effectiveness.

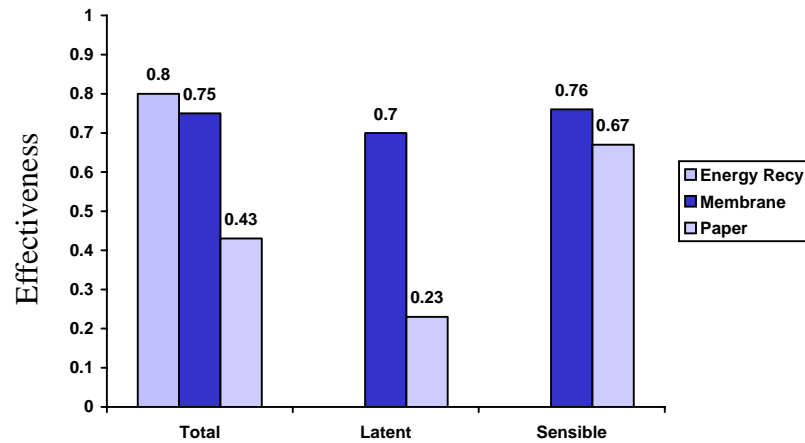


Figure 2.2. Effectiveness factors of current devices.

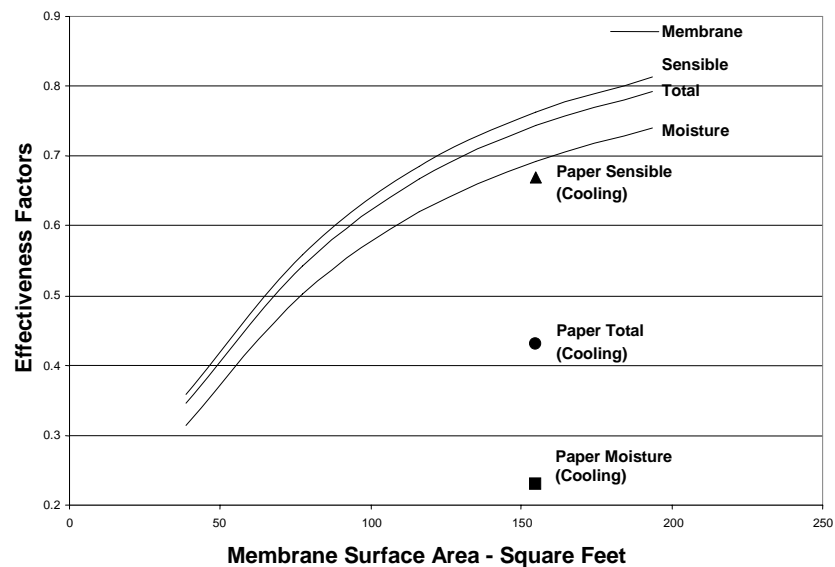


Figure 2.3. Comparison of membrane and paper core effectiveness as a function of size.

Heating and cooling ventilation air often account for 20% to 40% of the total HVAC energy used in commercial buildings. Numerous studies have shown the impact of increased outdoor requirement due to ASHRAE standard 62-1989 on the energy use and operating costs. A study done by Rengarajan *et al*, 1996, shows that the costs increased by 10 to 15% when a conventional chilled water variable volume system was used. The conventional system was also

unable to meet the increased latent load, resulting in elevated indoor humidity levels (i.e. numerous hours with relative humidity > 60%). The Rengarajan et al., 1996, study used an enthalpy recovery wheel with sensible effectiveness of 0.77 and moisture effectiveness of 0.77. The enthalpy wheels lowered both the cooling and heating loads on the HVAC system resulting in an almost 9% decrease in annual energy use. Additional fan energy required to overcome the airside resistance of the enthalpy wheel (311 Pa [1.25 in. w.c.] for both outside and exhaust airstreams) offset some of the energy savings. The savings for the proposed technology (enhanced ERV's) will be more because the pressure drop is very low (< 124.4 Pa [0.5 in. w.c.]), thus reducing the fan energy consumption. Using the energy saving number calculated in the study done by Rengarajan et al., 1996, the energy saving of ERV is 9%. Using the same number for EERV, and assuming a market penetration of 5%, the energy saving potential is $9\% \times (1.66 + 1.92) \times 5\% = 0.0162$ quads

The incentive to build tight residences that would require ventilation is highly dependent on energy prices. Recently approved ASHRAE Standard 62.2 establishes ventilation requirements in residences. Assuming the incentive to build tight homes is highest in the most northerly regions and most southerly (hot and humid) regions, it can be assumed that 10% of new homes would be built tightly in the most extreme climates. Over time this could be 10% of the building stock, making the savings $1.18 \text{ quads} \times 10\% = 0.12$ quads.

2.1. Experimental

The experimental program was broken up into three phases. Phase I involved membrane core optimization, preliminary enhanced energy recovery ventilator (EERV)/rooftop integrated design, a manufacturability study. Phase II involved modeling the performance of the integrated EERV/rooftop equipment and construction and testing of a demonstrator device. Phase III consisted of optimization studies, implementation, and testing of an optimized device. The experimental work with modeling support is outlined in chapters 7.0.

3.0 Membrane Core Optimization

During the course of this investigation several different types of experiments were conducted. During the first phase, various membranes were tested in an effort to assess their moisture transfer capability. This was accomplished by passing two separate gas streams (with an unequal moisture concentration across the membrane) flowing in a counter flow pattern across the membrane faces. Another aspect of the investigation was to assess the pressure drop occurring across various angled Lattice-Block-Module (LBM). Lastly, an attempt to assess whether the angled LBMs either enhance or degrade the heat transfer capability of the membranes was also attempted. Table 3.1. summarizes the membranes along with their general characteristics.

Table 3.1 Tested Membrane Summary

Membrane Type	Cross Linked	Sulfonation	Thickness (nm) (1mil = 25.4 nm)
0.125 Mesh	No	Low	50.8
	No	High	50.8
	No	High	25.4
Non-Woven	No	Low	50.8
	No	Std	50.8
	No	High	50.8
	No	High	25.4
	Yes	Std	50.8
None	No	High	50.8
	No	High	25.4

During this phase of the contract 11 different membranes with characteristics ranging from mesh type, cross-linking, degree of sulfonation and thickness were tested to determine their respective moisture transfer capability. Based upon the tests performed, a membrane with the following characteristics (ranked from most effective to the least effective) tends to promote moisture transfer:

1. High Sulfonation
2. 0.125 Mesh, then Non-Woven
3. Not Cross Linked
4. Thickness

For the various test performed, membrane #40 (0.125 Mesh, Not Cross-Linked, High Sulfonation, 2 mil) tended to provide the maximum amount of moisture transfer as compared with the other membranes.

Four different LBM designs were considered with the 45° angle design providing the lowest pressure drop. As a result, this LBM configuration was chosen for the prototype cores. Also, an

attempt was made to determine whether the presence of the LBM provides a positive or negative effect on the membrane moisture transfer capability. Although the results were inconclusive since the variation between tests with the LBM and without the LBM fell within the range of experimental variation, the presence of the LBM may in fact disrupt the boundary layer as theorized and thus reduce the resistance at the surface.

The design developed before this program started contained an interlayer separator part that replaced the corrugated design present in many air-to-air heat exchangers. In the corrugated design the air is trapped in each tube and there is no circulation between tubes. The Reynolds Number is so low that the device works like a laminar flow element and which makes boundary layer effects more dominant. Modeling suggested that the internal temperature and humidity gradients would be greater than if an open structure were used. This would help utilize all the membrane surface area. When even more expensive membranes were considered during an earlier period, it was even considered due to membrane cost to make a combination ERV/HRV in which sensible transfer occurred over a larger, mostly-non-membrane plate and a smaller area was reserved for moisture transfer with a membrane plate. The two functions of the shape selected were to (1) support the thin sheeting used for plates and keep them in position (i.e., avoid billowing), (2) and increase the homogeneity of the fluid field. The period of the structure was chosen to take advantage of “entrance effect” where boundary-layer thinning occurs in the region between turbulent flow and when it is becoming laminar. Each strut may act to “restart” this process and enhance the mixing. This potential heat transfer benefit may be traded off against the pressure drop created by the struts. Figure 3.1 shows two views of the LBM structure.

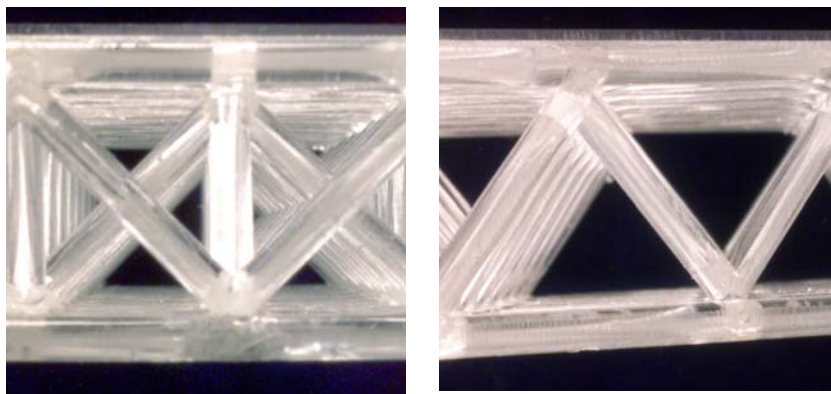
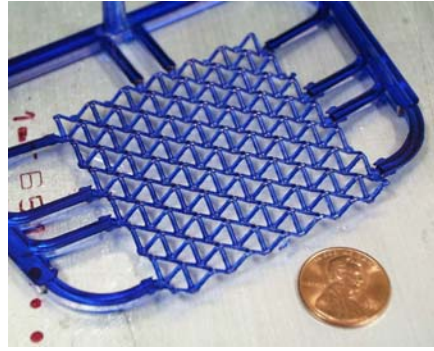
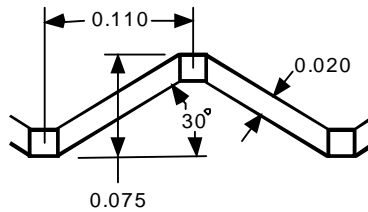


Figure 3.1. Lattice block structure. The orientation on the left is the “high-stirring/high pressure drop orientation”. The view on the right is the “lower-pressure drop/lower-stirring” orientation.

Shortly before the inception of this program, UTRC had worked with the LBM vendor to reduce the scale of the structure and thereby make it more appropriate for application to heat exchangers. Figure 3.2 shows the result. One further reduction was needed to meet the goals of this program.



(a)



(b)

Figure 3.2. (a) Demonstration small piece of lattice block structure at program inception. Blue dye was added to the plastic to increase visibility.

Assembly went well. Unfortunately, after producing 200 parts, the RenShape mold cracked from wear. This permitted only 50 layers to be produced. In order to keep the test window at the ARI certified test facility at Intertek/ETL-Semko (Cortland, NY), the stack had to be tested at this size. Constructing a new replacement mold, possibly out of aluminum would have delayed the program unacceptably.

Two rounds of testing were completed at Intertek/ETL. To test the subscale heat exchangers a flow rate of $\sim 1.13 \text{ m}^3/\text{min}$ (40 cfm) had to be used to keep the face velocity in the right range. Although data was obtained at this low flow condition, there were considerable difficulties maintaining the stability and accuracy of the facility at the low flow rate. Between rounds, the leaks were sealed as much as possible to remove this uncertainty. Better control of the facility at these flow rates would have allowed equalization of the internal pressure between the sheets and an estimate of leakless behavior could have been obtained. Some of the data received were encouraging in that they were near the design goals, but the degree of uncertainty was too large for them to be considered definitive. The sensible effectiveness is above the target of 0.76. The latent effectiveness is about 0.52 at an average airflow of $1.7\text{-}2.5 \text{ m}^3/\text{min}$ (60-95 cfm). Unfortunately, the facility was not able to get to the $1.06 \text{ m}^3/\text{min}$ (37.5 cfm) range that would have appropriate for the device. The high pressure drop in the test results is a result of the high flow through the device and the imbalances that resulted from the control systems desire to keep the supply pressure equal to the return pressure (position 2 = position 3). More plate area for this flow would have reduced the pressure drop proportionately. One of the contributing factors to the pressure drop may have been a result of construction difficulties in the counterflow entrance manifolds. The membrane spacer material should have done a good job keeping the plates separated inside the core, however, the torsion on the frames holding the membrane by the membrane itself created bowing in the entrances. As discussed before, this bowing is a result of

lack of humidity control by the membrane vendor during the manufacturing process and the frame had to prevent the membrane from curling.

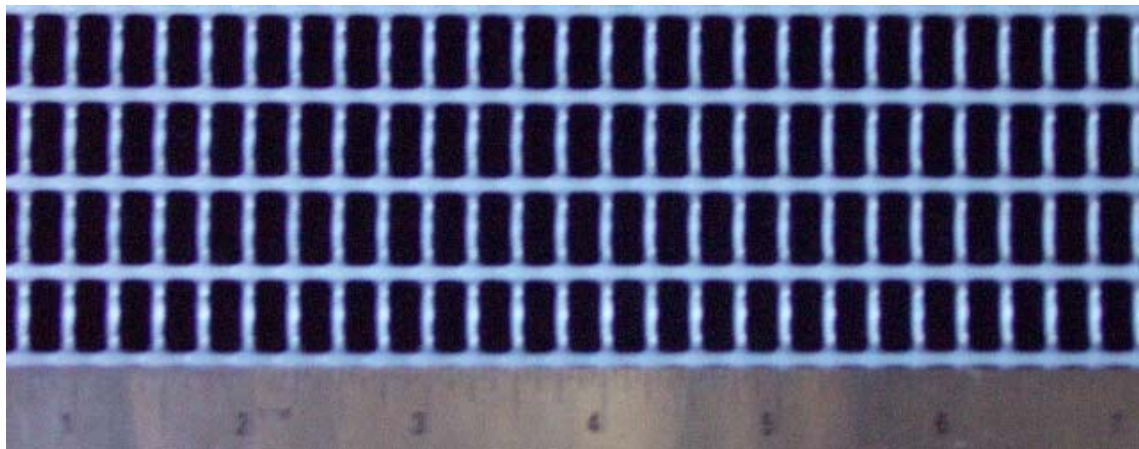


Figure 3.3. Photograph of the alternative mesh spacer

Due to production problems encountered with the full size mold for the LBM, a decision was made to stop this line of approach and use a spacer that might be lower in performance but which would be appreciably lower in cost and could be available on the time scale of the program and within the remaining resources.

A commercially-available roll mesh material was identified that could be used for spacers. Commercial off the shelf parts were also found which could be used as closure bars. Adhesives were identified that would permit hand assembly without leaks. The result of a performance benefits vs. cost projections led to the conclusion that a roughly 10% improvement in performance came at roughly a 10% increase in cost. It was decided therefore to build the full-scale EERV in industry-standard crossflow geometry.

A full scale heat exchanger was designed based on using this alternative mesh spacer (Fig. 3.3). Due to irregularity in the mesh it was decided to let the mesh float between the closure bars. These irregularities are a result of the inexpensive manufacturing process and there is no evidence that they will affect performance. Pieces of mesh were cut to fit just inside the closure bars with a minimal gap that accommodates irregularity. Polyethylene strips were used as closure bars. The strips obtainable in the time required had a height of 0.254 cm (0.1 in.), just higher than the height of the mesh itself. The closure bar strips were glued to the ends of the membrane plates and the mesh was laid inside the U-shaped channel. The stack was built by alternating the orientation of each layer. A stack of 200 layers was constructed. The total plate area of the device used was 109% of the area of the industry standard paper core that is used for comparison. This core was tested at Intertek-ETL at different flowrates and for both summer and winter conditions. The results are summarized in Table 3.2, and it can be seen that the performance objectives were achieved.

The core was then sent to the National Renewable Energy Laboratory (NREL) in Golden, Colorado, where further testing was carried out. They concluded that at ARI 1060 summer conditions the membrane core achieved sensible and latent effectiveness values nearly as high as that of enthalpy wheels. They also observed that the pressure drop on the supply side was very low, while the pressure loss on the exhaust side increased significantly as the flowrate increased.

This discrepancy was likely caused by a combination of the membrane deflecting due to the pressure differential between the two air streams and the ribbing support structure transverse to the air flow.

A second core was then built with thinner closure bars. The polyethylene strips used had a height of 0.203 cm (0.08 in.), just thinner than the height of the mesh itself. The core was sent again to NREL and they observed a substantial improvement over the original design, with a 25% decrease in average pressure drop and a 5 – 10% increase in effectiveness. The tests also indicated that the sensible effectiveness was independent of humidity and that the latent effectiveness is not affected by the humidity ratio potential as predicted by convective mass transfer theory. On the other hand, the latent effectiveness increased by approximately 25% with an increase in average inlet humidity ratio from 65 grains/lb to 120 grains/lb.

SF₆ leak tests were carried out at UTRC after the unit was returned. No measurable leak was observed. The shipping process and airflow testing did not create any apparent leaks in the leak tight device.

The effectiveness of a heat exchanger depends strongly on the flow rate. The program goals are indicated showing that the goal effectiveness was reached at the high end of the intended flow range. Table 3.2 summarizes the Phase I goals and the test results. Cost and size are discussed in the Manufacturability Study (Section 5).

Table 3.2 Performance Goals and Results

Performance Attribute	BP1 Goal	Paper Core Standard	Results
Latent Effectiveness (ARI 1060)	0.70	~ 0.22	met at ~70.3 lps (~149 scfm)
Pressure Drop	< 125 Pa (0.5 in w.c.)	125 Pa (0.5 in w.c.) at 70.3 lps (149 acfm)	50 Pa (0.2 in w.c.) at 70.3 lps (149 acfm)
Sensible Effectiveness (ARI 1060)	0.76	0.76 at 56.6 lps (120 cfm)	met at ~69.9 lps (~148 scfm)
Exhaust Air Recirculation	0.03	~0.03	no measurable leak
Cost	~\$1.18/layer	~1.18/layer	~\$0.86/layer
Size	1.67-2.5 lps/l (100-150 cfm/ft ³)	1.67-2.5 lps/l (100-150 cfm/ft ³)	~2.5 lps/l (~150 cfm/ft ³)

4.0 Preliminary EERV/Rooftop Integrated Design

The purpose of this design effort was to do a preliminary design of a rooftop integrated EERV so that the dimensions chosen for the full-scale heat exchanger are acceptable for integration. The design process consisted of selecting an existing rooftop, and the 50HJ004 unit (High Efficiency “Weathermaster”) was selected as the most relevant model. A design was selected where the core would sit where the economizer option would normally be attached, at the side of the air inlet plenum.

A transient model was developed to both study the effects of the EERV on the rooftop performance, and as a precursor to the future control design in Phase II. In its present form it can integrate over a full year with 5 minute time steps in 13 seconds on a standard PC. Typical Mean Year (TMY) hourly data was used for the analysis. Three cities were chosen to represent different environments:

- Miami: Hot and humid,
- Phoenix: Hotter but dry, and
- Boston: Northern.

Nine cases were run to study how ventilation and an EERV affect yearly energy cost. For each of the three cities, the following three cases were run:

1. No ventilation: This is the baseline for when there is no ventilation load. This case has the lowest energy consumption. (Since not humidity load was added to the zone, the entire load on the rooftop unit is sensible.)
2. Normal ventilation, no EERV: This is the normal case for which the rooftop unit and heater were sized. This case has the highest energy consumption.
3. Normal ventilation, with EERV: The addition of the EERV removes much of the load that the ventilation adds. This case consumes an amount of energy between the other two cases.

Figure 4.1 shows the energy consumed for the nine cases described above. Note that the Boston case consumes far more energy than the other two. This is for two reasons.

1. The zone is larger, since it was sized to match the cooling capacity of the rooftop unit, which can handle a larger zone in the cooler climate, and
2. It is dominated by the heating load, which is being met inefficiently by an electric heater.

Figure 4.2 shows the same data normalized to the “No EERV” case. For all three test cases

- Ventilation contributes between 43 and 35% to the base load (without EERV), and
- The EERV saves between 19 and 30% of the base load.

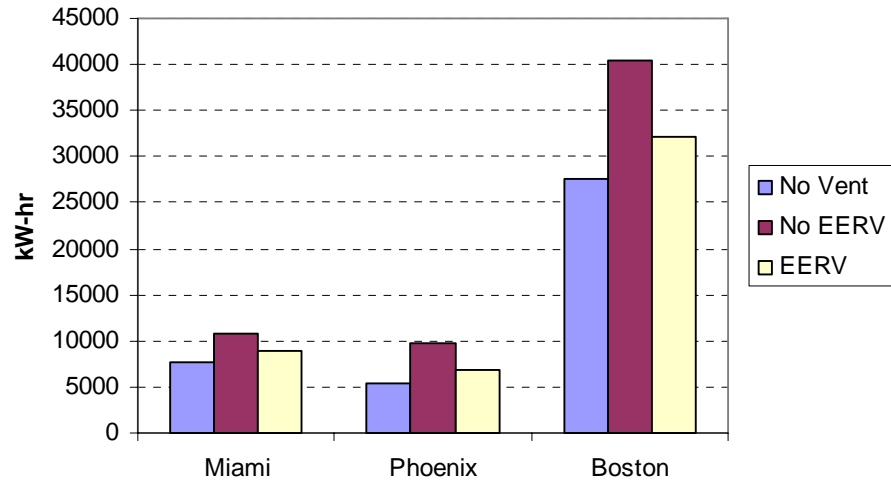


Figure 4.1. Consumed energy with and without EERV for three cities.

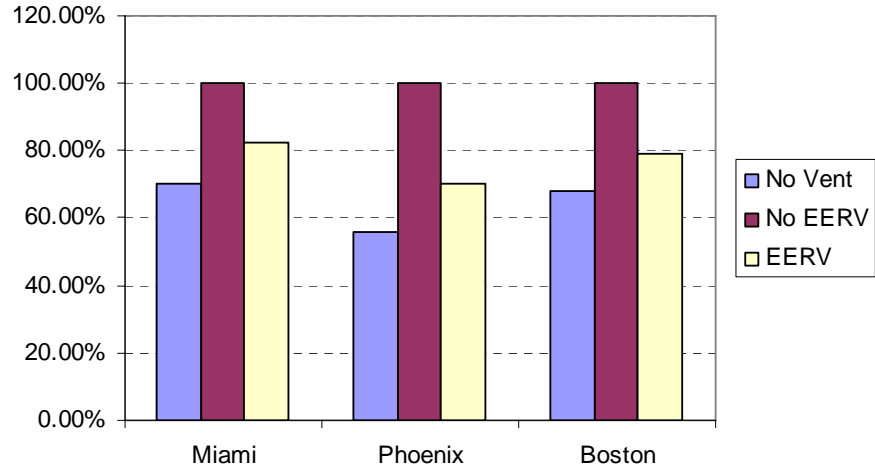


Figure 4.2. Energy usage with and without EERV for three cities normalized to the no EERV case.

5.0 Manufacturability Study

To understand the cost of producing the units as a function of annual manufacturing quantity, it was necessary to develop a better understanding of what a production line might consist of, what the price of components and materials would be as a function of quantity purchased, and what the cost of labor and machines might be for assembly and testing. To this end a manufacturability study was conducted by the Center for Automation Technology (CAT) at RPI. During this investigation, the CAT conducted a study of alternative manufacturing and assembly processes for the components of the EERV and developed a new, manufacturable product design. Estimates of the EERV components costs and manufacturing systems costs were also developed.

The following specific activities were involved:

- An analysis of the proposed costs by the membrane supplier
- An analysis of the proposed costs by the LBM supplier.
- An analysis of alternative EERV designs.
- Recommendations on design features to improve manufacturability, leading to a completely new design.
- A proposed assembly sequence.
- A proposed assembly plan, including equipment and labor required.
- An estimated assembly time.
- Estimated unit costs at various volumes.

Six alternative designs to the cross-flow design originally developed by UTRC were analyzed to examine how effectively the membrane was utilized. In both cases, assumptions were made on EERV dimensions. The six alternative designs are:

Counter-Flow Plate Design
Counter-Flow "Fan Fold" Design
Counter-Flow Coil Design
Cross-Flow Cardboard Frame Design
Cross-Flow "Air Pillow" Design
Cross-Flow Tubular Design

An analysis of the alternative designs was conducted

In the first comparison, the ratio of the area of membrane that is exposed to the air streams for heat transfer to the total volume occupied by the EERV is plotted against the ratio of area of membrane exposed to the air stream to the membrane consumed in making the EERV. Points higher on the plot indicate designs that more efficiently use the membrane with respect to the EERV volume consumed, and points further to the right indicate designs that more efficiently expose the membrane to the air stream (less waste). This is shown in Figure 5.1.

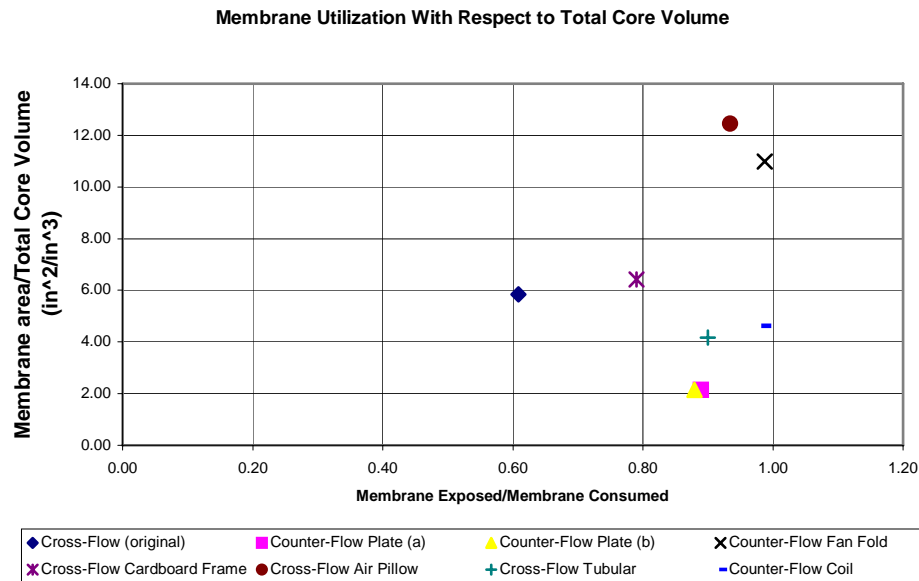


Figure 5.1. Alternative design comparison: membrane utilization with respect to total EERV volume.

Figure 5.2 is similar to Figure 5.1 except that the active EERV volume is used instead of the entire volume, where the active volume is defined as the volume of the EERV where energy transfer takes place. Similarly, designs that fall to the upper right of this plot indicate most efficient use of the membrane and the space consumed by the EERV.

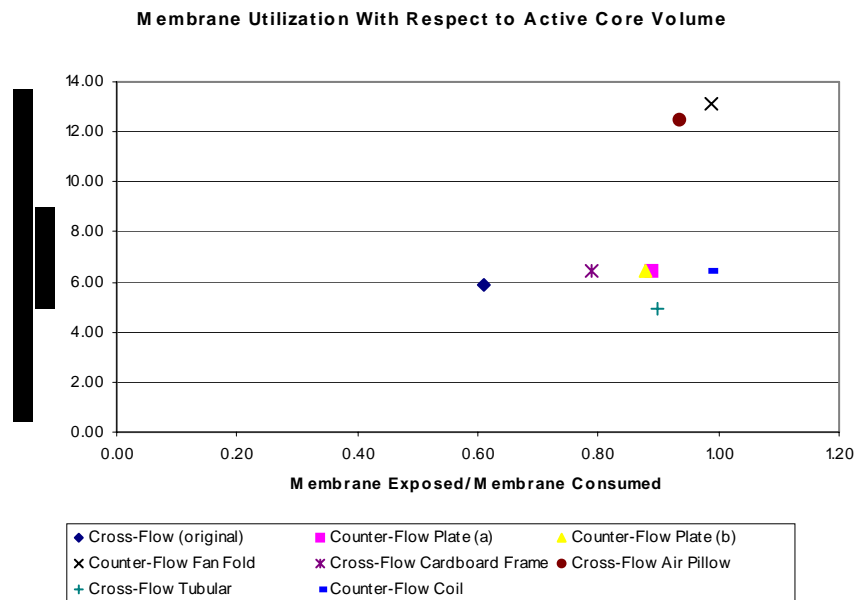


Figure 5.2. Alternative design comparison: membrane utilization with respect to active EERV volume

In both Figs. 5.1 and 5.2, the Cross-Flow Air Pillow and Counter-Flow Fan Fold designs appear near the upper right corner, making them the designs with the greatest efficiency. The Cross-Flow Air Pillow design was rejected because of concerns associated with the movement of the Membrane inside the core when subjected to pressure differentials in the two air streams. Without a rigid structure to maintain an air space between adjacent Membranes, pressure differentials could cause the air spaces on the lower pressure side to collapse, thereby reducing the air flow, aggravating the pressure differential and reducing the heat transfer. Other cross-flow designs were rejected because of the improved heat transfer efficiency obtainable with a counter-flow design.

Among the counter-flow designs, the Tubular design was rejected because of complexity. The Counter-Flow Fan Fold design, while exhibiting more efficient use of the Membrane than the Counter-Flow Plate designs with respect to the overall volume of the core, the two designs show roughly the same amount of Membrane waste. Since minimizing Membrane waste was deemed more important than efficient use of overall space and the manufacturing processes associated with the Fan Fold design were found to be more problematic than those associated with the Plate designs, it was rejected. Thus, the Counter-Flow Plate design was selected as the design with the best combination of manufacturability and efficiency.

EERV Design Concept

After analysis and several discussions concerning the strengths and weaknesses of the alternative EERV designs, the CAT and UTRC concluded that the Counter-Flow Plate Design offered the best combination of performance and manufacturability. Further discussions about how best to configure the design so that it can be installed into an existing rooftop unit for the demonstration phase of the project lead to changes in the shape of some of the components. Using this information, conceptual designs of the individual EERV components were completed.

EERV Costing Estimate

The purpose of the cost estimating conducted was to establish reasonable expectations for the unit cost of an EERV based on the materials, labor and overhead that go into producing it. The cost estimation is not an investment analysis, so the time value of money has not been taken into account as this falls outside the scope of this project. Additionally, estimates of the costs for capital equipment to manufacture the EERV are included to facilitate an investment analysis, but have not been amortized herein.

All overhead costs normally associated with a manufacturing operation (lease, utilities, shipping, inspection, maintenance, taxes, insurance, etc.) are factored in by application of an overhead rate (20%) to the Direct Materials and Unburdened Direct Labor costs. Non-production overhead costs such as marketing research, advertising, R&D etc. have been ignored under the assumption that the EERV manufacturing will be too small to support them. The cost of borrowing funds has been ignored.

The total unit cost of an EERV is the sum of the material cost per unit, the burdened assembly labor per unit and the overhead. In general, the unit cost of each of the materials is a function of the quantity produced.

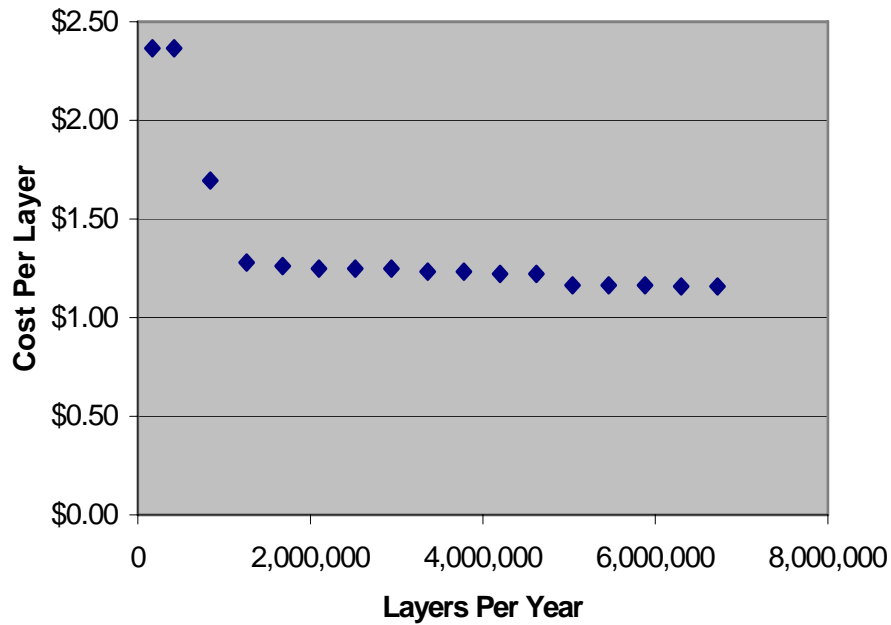


Figure 5.3. Cost per layer vs. layers per year.

Figure 5.3 shows the cost per layer vs. annual production (layers/year). At an annual volume of 40,000 EERVs, the total cost of an EERV with 168 layers, making it roughly comparable in size to the existing paper core, is:

$$\text{\$1.16} * 168 = \text{\$194.88}.$$

The cost breakdown of the EERV at this volume is shown in Table 5.1 and Fig. 5.4.

Table 5.1 Cost Breakdown at 40,000 EERVs Per Year

Cost Percentages (40,000 EERVs/yr)	
Membrane	42%
LBM Spacer	23%
Overhead	17%
Frame	14%
Angle Spacer	3%
Direct Labor	2%

Cost Breakdown at 40,000 EERVs

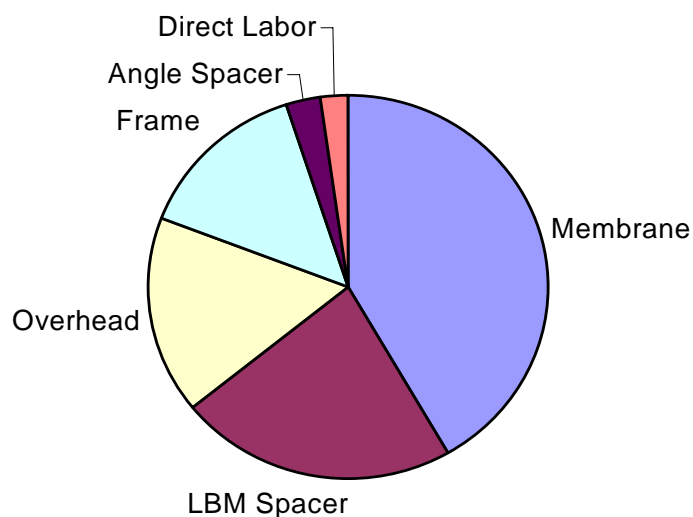


Figure 5.4. Cost breakdown at 40,000 EERVs per year.

The change in spacer design described in Section 3 and change to a crossflow configuration has beneficial cost impacts that are estimated in Table 5.2. This lowering of projected manufacturing cost will permit the technology to access wider regions.

Table 5.2 Implications of Design Change on Projected Manufacturing Cost

	Original Design		Improved Design		Change
Cost Element	Cost per cfm	%	Cost per cfm	%	%
Membrane	\$ 0.49	42	\$ 0.49	49	0
Spacer	\$ 0.27	23	\$ 0.16	16	-11
Frame	\$ 0.16	14	\$ 0.00		-16
Angle Spacer	\$ 0.03	3	\$ 0.00		-3
Direct Labor	\$ 0.02	2	\$ 0.02	2	0
Overhead	\$ 0.19	16	\$ 0.22	19	0
Total per Layer	\$1.16	100	\$ 0.86	100	-30

6.0 Modeling the Performance of Integrated EERV/Rooftop Equipment

In order to improve the design of the demonstrator unit and improve the knowledge of customer benefits of an integrated unit, a simulation development task was undertaken that involved teaming with the Center for Building Performance and Diagnostics (CBPD) in the Architecture Department of Carnegie Mellon University. CBPD has a long history of applying building energy simulation methods to design problems, and they developed test models for simulation runs of different HVAC system configurations with and without an EERV unit. An advanced energy simulation tool was used to compare the performance of packaged, rooftop HVAC equipment. The objective was to model a typical office building with multiple system configurations in multiple climatic zones in United States to evaluate the performance of energy recovery technologies in packaged rooftop HVAC equipment. The system configurations that were modeled – base line, economizer, energy recovery ventilator (ERV) and bypass – were analyzed with respect to system sizing, indoor design conditions (temperature and relative humidity), annual average coil runtime fraction, annual average coil sensible heat ratio (SHR) and system annual energy consumption.

The approach used for this study was to conduct background research to determine the most typical application for packaged, rooftop HVAC equipment by building type and occupancy. The data revealed that 32% of cooled buildings in the United States are between 929 – 9,290 m² (10,000 – 100,000 ft²), that 21% of cooled buildings are office occupancies and of these, 57% use packaged rooftop HVAC systems.

To select the appropriate simulation package for this study, the features of the traditional DOE 2.1 application with those of the newer EnergyPlus software were compared. EnergyPlus was selected because it provides a user-definable time step for building and system simulation and it can model the latent-load degradation performance of the DX cooling coil under part-load conditions. EnergyPlus input files were created for sixteen configurations for an office and a single city. The combinations represent four sizes of cooling capacity, a single size of heating capacity, the presence of an economizer option or lack thereof, and the presence of an EERV or lack thereof.

The final building model that was simulated was a mid-level, corner office zone of 9m x 12m x 4.2m (29.5 ft X 39.4 ft X 13.8 ft) in Miami, FL with five HVAC configurations:

- standard constant air volume (CAV),
- CAV with economizer,
- CAV with ERV,
- CAV with ERV and economizer,
- CAV with ERV and bypass.

An objective of this study was to understand the effect of ERV on annual energy consumption, annual average coil performance and resulting indoor thermal conditions. The results of this study indicated that for a fixed DX coil size (18 kW), the annual energy consumption of a standard CAV package compared to the energy consumption of a CAV package with an ERV and a bypass configuration was reduced from 14,634 to 13,576 kWh, or 7.2% for Miami, FL. The number of hours that the indoor temperature setpoint is not met was reduced from 327 to 43 hours, an 87% improvement. The number of hours that indoor relative humidity was unacceptable (above 60%) was decreased from 1518 to 1242 hours, an 18% improvement.

Another objective of this study was to better understand the impact of system sizing in varying configurations on system energy consumption and indoor temperature and relative humidity conditions. The results illustrate that as system size is increased, the number of hours that the indoor temperature setpoint is not met decreases, while the number of hours that the indoor acceptable relative humidity range of 30% - 60% is not satisfied increases. With respect to a fixed number of hours wherein the indoor temperature setpoint is not met (130 out of 2600 hours during occupied periods within a year), the results indicate that the inclusion of an ERV with a bypass configuration compared to a standard CAV system would enable a size reduction from 19.3 to 16.6 kW, or 14%.

Geographic Survey of U.S. Cities

In order to better understand

(1) the value proposition for the nation, for the customer, and for the manufacturer and to identify the associated building types and markets where this equipment is most likely to be beneficial, and

(2) the internal details of operation, that could not be instrumented and measured, for the purpose of assisting the design of product components and controls

a wide geographic analysis was needed. The customer value proposition for energy recovery devices used was evaluated with downsized cooling equipment. From a manufacturer perspective, the size of the markets for the type of building must be quantified to know potential production quantities and costs of manufacture in those quantities.

It was found that the latest version of EnergyPlus has a batch run facility that is capable of running unattended a list of simulations. A list was created for 62 U.S. cities for which weather data was readily available. For each of these there were 16 configurations, resulting in 992 simulations for each “case”. A case is a particular building type with a specific outside air ventilation rate. Scripts were created to post process the 992 Excel output files into plots and tables for further examination. Since about 30 styles of plot are produced for each city, about 1860 plots are created and kept on file for each “case”. The sixty-two locations were chosen that represented a wide range of climate, included most major cities of economic importance, and had at least one city in every state. For the purposes of reporting, Miami and New York were selected for display. The former represents a “hot and humid” climate and the latter a balanced seasonal climate with significant cooling and heating seasons.

For this series the sensible-heat ratio was kept constant at 0.68 which is typical of much of the equipment currently in the marketplace. Also, in the small capacity range, it is not possible to downsize a unit to an arbitrary size that would represent right-sizing after addition of an EERV. Hence a single cooling downsizing was adopted for this initial study. This might be the perspective of a national-account type of customer who buys only a few model sizes to equip facilities over a wide geographic area.

The initial size was the largest of the units the input files were set up for, 21.6 kW (5.86 TR), in order to check agreement with results obtained at CMU. The downsized unit was 18.0 kW (5.12 TR), or about 17% which may be appropriate for many situations. These initial choices were made for convenience in error-proofing code. The automatic simulation system described below permits the group of runs to be rerun and the results processed automatically.

The batch process runs the 992 simulations in about 24 hours on an upper-end desktop PC. The output files are the 992 Excel spreadsheets that contain hourly results. The output columns selected by CMU were augmented to include the psychrometric conditions at all the node points of the system. It is important to note when looking at the data that each value represents an average during the hour. Unless an hour is chosen that has 100% duty cycle, the values given will not match the performance curves for a unit in steady state.

To avoid laborious manual processing of the spreadsheet results, scripts were written in MATLAB to read in the .csv files and process them. About 30 types of graph are produced for each of 62 cities; these .jpg files may be stored and recalled for later observation. The wide climatic differences tend to provoke different phenomena, so it was an iterative process of observation and improvement to the EnergyPlus input files to get a situation that gave intuitively correct behavior over the collection of cities.

Postprocessing of the EnergyPlus output files also led to the creation of new Excel spreadsheets that summarized annual behavior by city, e.g., the percent of energy saved and other aspects of interest. Since city longitude and latitude were incorporated into these files by the MATLAB scripts, these new data files may be read by Golden Software MapView software that can produce national maps of the property.

Main results for Miami and New York are summarized here:

- The downsized system with EERV delivers equivalent roughly equivalent cooling to the larger standard system without EERV.
- The downsized system with EERV requires significantly less peak power than the larger system without EERV. In areas where demand charges are applied this can result in a significant monetary savings to the customer. The utility would also need lower installed generation capacity for this customer.
- The downsized system with EERV has a higher effective COP. Improvements to controls to reduce the number of hours with low COP are under investigation. These may be mostly hours with short cycles due to low cooling needs.
- The downsized system with EERV has a lower SHR for many hours, which would lead to better humidity control. A SHR of 1 means no latent removal or a dry coil situation. The coil SHR was 0.7. The average hourly value was computed by examining the effective overall sensible heat removed in relation to the total. In hours when the SHR=1 the coil was effectively dry.
- The range of conditions presented to the evaporator and heating coils for the EERV case is narrower than for the non-EERV case. For Miami the overall moisture into the coil is also lower, leading to the possibility that a thinner and lower pressure drop evaporator coil could be used.
- The EERV supply output is affected not only by the outside air but also by the return air conditions. The “weather compressor” attribute of the EERV is obvious from the narrowing of the distributions. The “weather compressor” property is noticeable even at 38% outside air. The preprocessed outside air entering the mixing plenum upstream of the coil covers a narrower and milder set of conditions than for direct outside air.

- While there is virtually no heating in Miami, for New York, the heating system operates at full power much less often when the EERV is present.
- The extended cooling season in Miami relative to New York is apparent as is the fact that both systems deliver roughly equivalent cooling.
- There is a modest energy penalty for over sizing the system due to short cycling.
- As the system becomes undersized the ability to hold the cooling set point is diminished.
- The modest effect of the economizer is apparent.
- The greater percentage energy savings for New York is due to the presence of a heating season. For New York a bimodal distribution indicates the prevalent conditions during cooling and heating seasons.
- For Miami the overall moisture into the coil is also lower, leading to the possibility that a thinner and lower pressure drop evaporator coil could be used.
- There is a tight control of temperature in the conditioned space for most hours. The lack of humidity control is comparable for both systems, but with the EERV equipped system it is slightly better.

Preliminary Evaluation of Bypass by Simulation Postprocessing

In the current EnergyPlus model, the system supply fan stays on continuously. Assuming that the supply fan is the only fan available to move ventilation air, independent of whether there is an EERV present, in a more realistic system the supply fan would be off during unoccupied hours when ventilation is not required and there is no call for heating or cooling during the setback period. Future versions of EnergyPlus may permit this option. In the meantime, an estimate may be made subtracting this fan energy from the energy cost during hours when it should be off. If the fan motor is in the airflow this would also require removal of fan heat from the air stream. During the heating season the fan adds heat that doesn't have to be supplied by direct heating. During the cooling season the fan adds heat that must eventually be removed by the cooling coil, or if the night outdoor temperature is low enough by conduction through the walls.

In the current EnergyPlus model, the supply fan energy usage is 11.6×10^5 J/hr when the EERV is present. When the EERV is not present, the supply fan energy is 9.56×10^5 J/hr. The difference is presumably due to the additional fan power required due to the pressure drop of the supply leg of the EERV. This difference is 2.0×10^5 J/hr. The exhaust fan used to move return air through the exhaust leg of the EERV in the current model is 0.92×10^5 J/hr, or a factor of 2.2 smaller. If the two fans had the same efficiency and the mass flux through a balanced EERV were equal, one would expect the incremental supply fan energy to equal the exhaust fan energy. On the other hand, since large fans are usually more efficient than small fans, one would actually expect the supply fan energy to be lower than the exhaust fan energy. Some model changes may be needed to address this effect.

An ad-hoc post-calculation was done for New York results to get an approximate evaluation of the benefit of EERV bypass. This would serve as a guide to the amount of future effort to place on it. In this brief study the baseline standard-sized system without EERV was compared to a downsized system with EERV and to a downsized system without EERV. For any hour where

the reduction heating or cooling energy for the downsized system with EERV did not exceed the corrected EERV fan energy, the results from the calculation for the downsized system without EERV was substituted for that hour. This ignores the fact that the initial conditions for the state of the system at the beginning of the hour might be slightly different. Proceeding with this approach let to an estimate for cooling energy savings that was 28% higher than that obtained by using a downsized system with EERV but without bypass.

Predicted Energy Savings

The modeling results obtained city-by-city was expanded to about 100 cities and assembled using a map visualization software to show the benefits of this technology as a function of climate region on a national map. In a sample problem, a packaged unitary (rooftop) system was downsized from about five tons to about three tons. The sample office building was a size that is consistent with using about five tons of cooling without energy recovery. Fig. 6.1 shows by city the annual energy savings for each of the individual cities. This is a lower bound since a bypass option was not considered in these calculations. Fig. 6.2 shows an approximate interpolation between cities based on the data in Fig. 6.1. Clearly while the savings with EERV occurs during the long cooling seasons in hot and humid climates, much of the benefit of EERV units will come during long heating in northern latitudes where the indoor-outdoor temperature difference is on average larger.

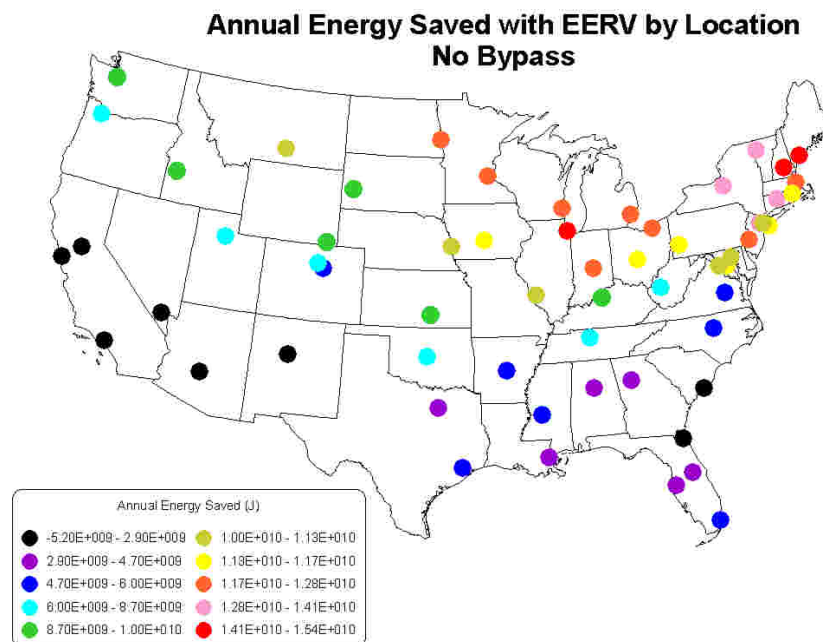


Figure 6.1. National map of annual energy savings by location with an enhanced energy recovery ventilator with a packaged unitary HVAC unit using a fixed downsizing.

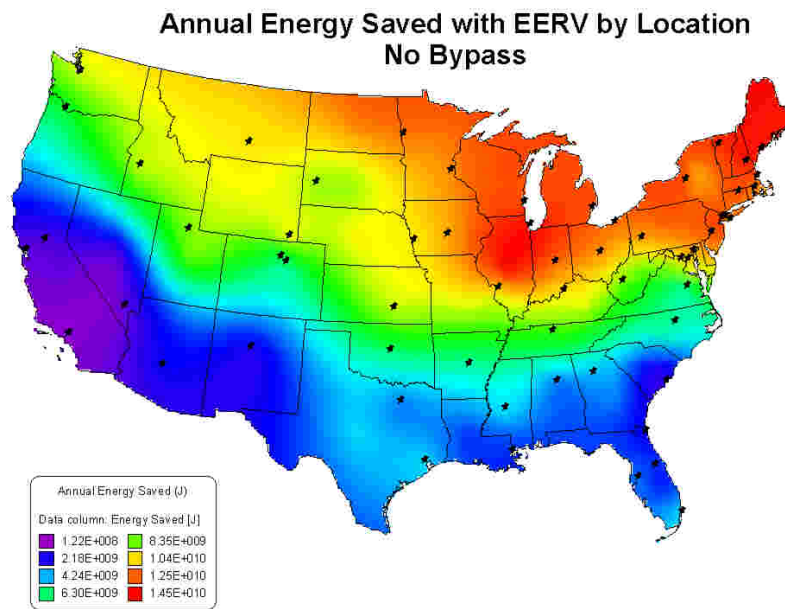


Figure 6.2. Interpolated representation of the same data displayed in Figure 6.1.

7.0 Integrated Packaged Unitary EERV-Rooftop Demonstrator

The primary goal of Phase II was to create a demonstrator unit that integrates an EERV with a packaged unitary rooftop unit and test it. This included the associated controls. The goal was to demonstrate that the energy recovery expected from the core optimized in Phase I was obtained while learning additional performance characteristics that will be useful in Phase III Optimization.

Figure 7.1 shows a schematic of the integrated EERV-rooftop unit. This arrangement is suitable for installations with horizontal return and supply ducts. A standard Carrier Horizontal Economizer option was purchased and installed in the mixing plenum. The economizer contains two sets of dampers. One set blocks the return air from the mixing plenum, while the other opens up to the outside air. The former was maintained and used as the “recirculation air damper”. One of the two damper-blades of the outside air damper was removed to allow the fresh air from the EERV into the mixing plenum. The other damper-blade was initially maintained as the bypass damper. This was later moved to an upstream location in the fresh-air bypass duct.

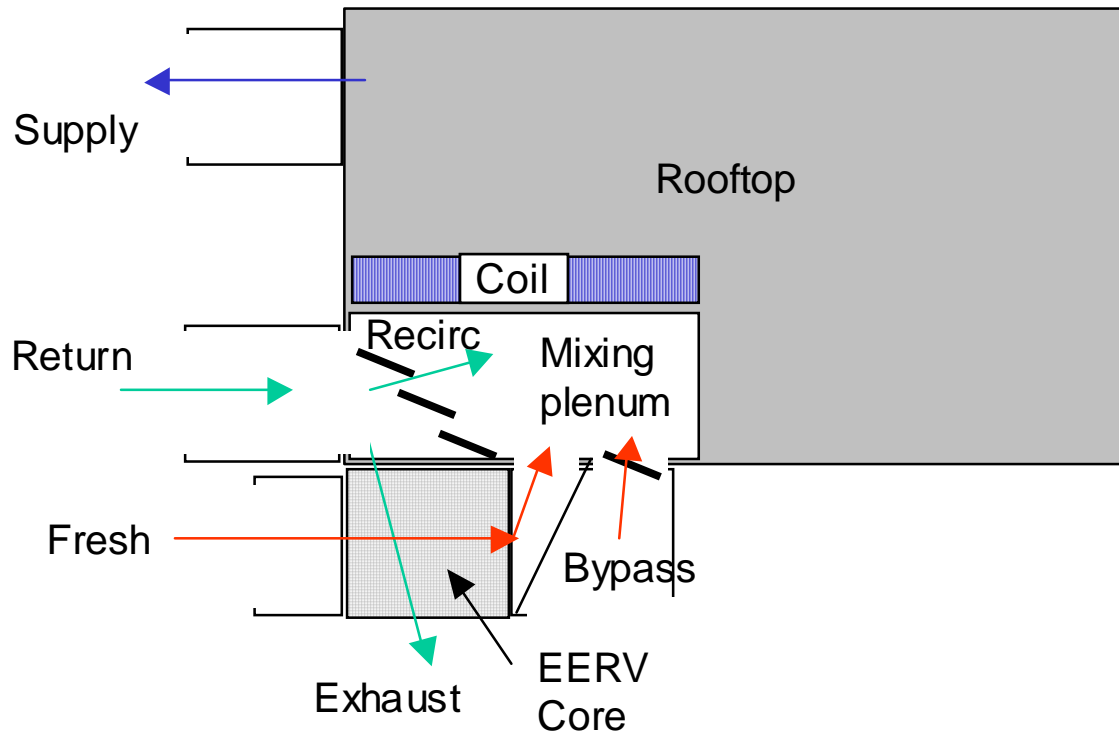


Figure 7.1. Rooftop schematic of EERV/rooftop integrated system.

There are 5 separate air flows associated with this arrangement. They are defined in the Table 7.1.

Table 7.1. Integrated System Airflows

Name	Parameter/Equation	Example values
Supply	Q	1200 scfm
Return	$f1*Q$	1200 scfm ($f1 = 1$)
Fresh	$f2*Q$	360 scfm ($f2 = 30\%$)
Recirc	$\text{Supply} - \text{Fresh} = (1-f1)Q$	840 scfm
Exhaust	$\text{Return} - \text{Recirc} = (f2-f1)Q$	360 scfm

Of these five, only three are independent. All five flows can be defined by:

1. The supply air flow rate, Q
2. The ratio of the return air flow rate to the supply, $f1$. An $f1$ of 0.9 allows for building pressurization and makeup for exhaust fans.
3. The ratio of the fresh air to supply, $f2$. Typically 0.2 to 0.4.

Bypass is considered to be part of the Fresh flow, although it is not conditioned by the EERV.

An exhaust fan was used to produce the exhaust flow. For the demonstration unit, the pressure in the mixing plenum was used to pull the fresh air flow.

The core assembly is shown in Figure 7.2. For the horizontal duct arrangement the core is stacked vertically. The core was placed in an Acrylic box. Its edges were sealed to prevent leakage. The core dimensions are 11.5" X 11.5" X 36" high. It is a cross-flow design where the air enters the stack on the 11.5" by 36" sides.



Figure 7.2. EERV core assembly for demonstrator unit.

Test Facility Description

A test facility was built for this project for this project using UTRC capital funding. It consists of two main chambers illustrated in Figure 7.3:

1. Humidity Chamber, and
2. Outdoor Chamber (which contains the rooftop and EERV assembly).

In addition to the above two chambers, air could be exchanged with the ceiling plenum over the test rooms. The list of measurement stations is summarized in Table 7.2. Temperature (T) and relative humidity (R) were measured at each station; flow (F) was measured at three of the stations. Pressure was also measured at the following stations:

1. Across the fresh air stream of the EERV
2. Across the exhaust air stream of the EERV
3. Between the mixing and condenser chambers.
4. Between the humidity and condenser chambers.

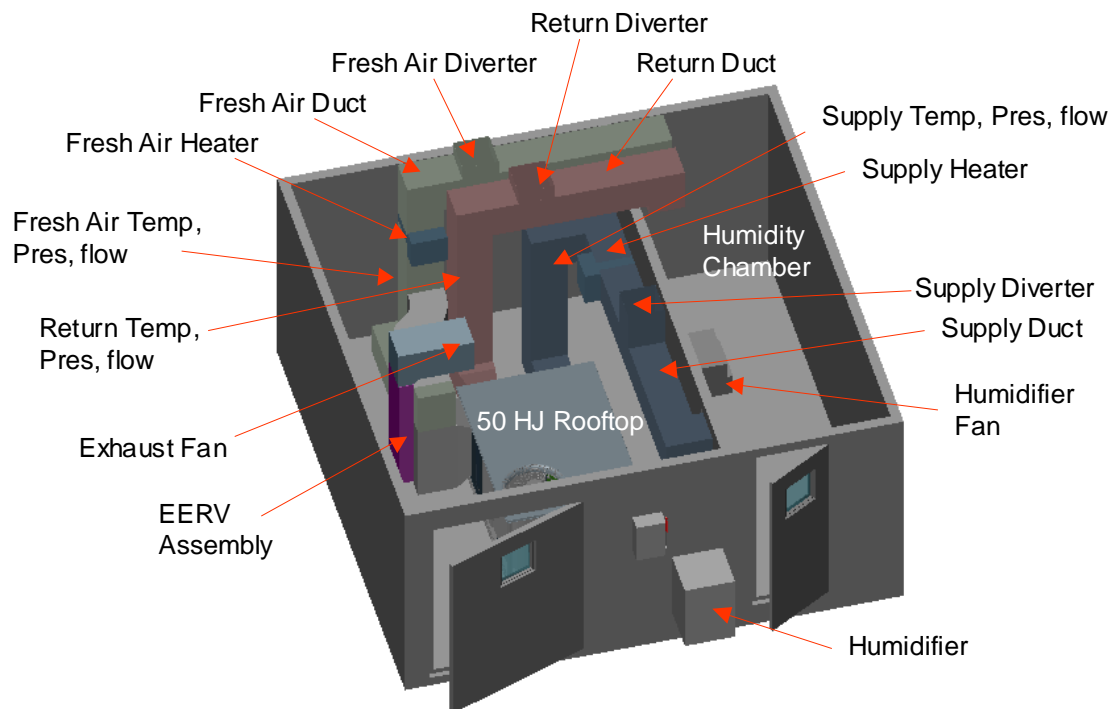


Figure 7.3. Test facility schematic.

Table 7.2. List of Measurement Stations

	Name	Description	T	R	F
1	Supply	Supply duct from rooftop	Y	Y	Y
2	Return	Mixed air return duct to rooftop	Y	Y	Y
3	Fresh	Mixed air for EERV and bypass	Y	Y	Y
4	EERV	Fresh air output from EERV	Y	Y	
5	Exhaust	Stale air (from return) output from EERV	Y	Y	
6	Condenser	Zone condition that houses rooftop	Y	Y	
7	Humidity	Humidity chamber room	Y	Y	
8	Plenum	Ceiling plenum above chambers	Y	Y	

Table 7.3 describes the facility and test unit actuators.

Table 7.3. List of Facility and Test Unit Actuators

	Name	Description
1	Supply damper set	Two dampers that can direct the supply air flow to either the ceiling plenum or the humidity chamber
2	Return damper set	Two dampers that can mix the return air from the ceiling plenum and the humidity chamber.
3	Fresh damper set	Two dampers that can mix the fresh air from the ceiling plenum and the humidity chamber.
4	EERV bypass damper	Damper that can open up the bypass flow. Since it has much less pressure drop than the EERV, when it is open most of the air flow bypasses the EERV.
5	Exhaust fan	Pulls air from the return duct through the EERV and out into the condenser chamber. For the purpose of the demo it was varied with a variac. For the actual product it may be on/off or variable depending on the cost trade-offs.
6	50HJ rooftop	Test unit
7	Humidifier	Provides humidity and heat to the humidity chamber
8	Supply air heater	Re-heats the supply air. Cancels the cooling capacity as needed. May be used to control the humidity zone temperature.
9	Fresh air heater	Heats the fresh air after it is mixed to simulate hot outdoor temperatures.
10	Recirc Air damper	Actually a modified Carrier economizer damper. Produces a pressure drop between the return air and the mixing plenum in the rooftop. Used to control the fresh air flow rate.
11	10-ton rooftop unit	Used to control the air temperature of the condenser chamber. The air entering the condenser should be the same temperature as the fresh air, but may differ in humidity for testing purposes.

Test Rooftop and EERV Core Description

Figure 7.4 shows the installation in the outdoor room. Visible in this view are the 50HJ 3-ton rooftop unit, the EERV core in an acrylic box standing to its left, the exhaust duct and fan, and the fresh-air bypass. In an integrated product the fresh air ducts would not be necessary since the fresh air would be coming directly from the outside ambient. Also, the exhaust fan could be located right on top of the EERV stack. Additional facility views are shown in Figure 7.5.

Facility Controls

Facility and EERV controls were implemented using a Carrier CC6400 programmable controller with two expansion IO modules (Figure 7.6).

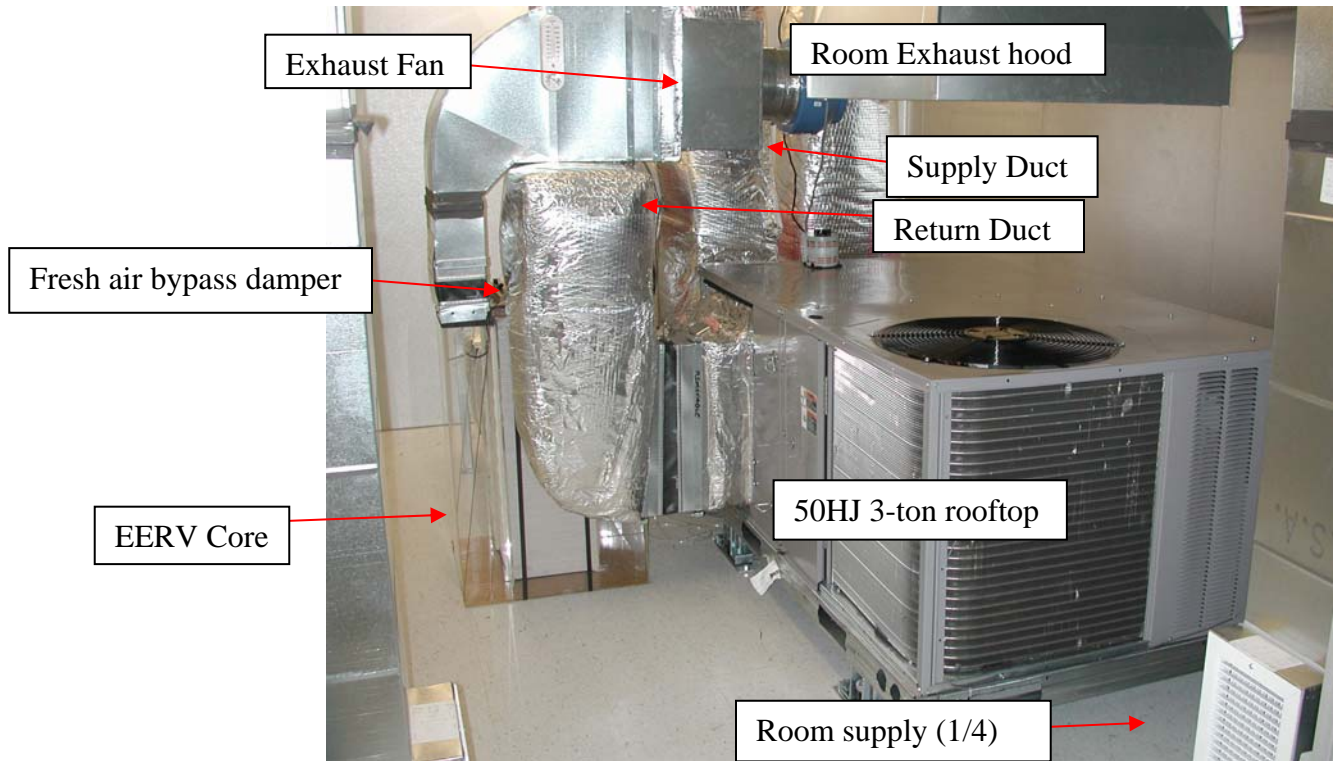


Figure 7.4. View of test hardware in outdoor chamber.

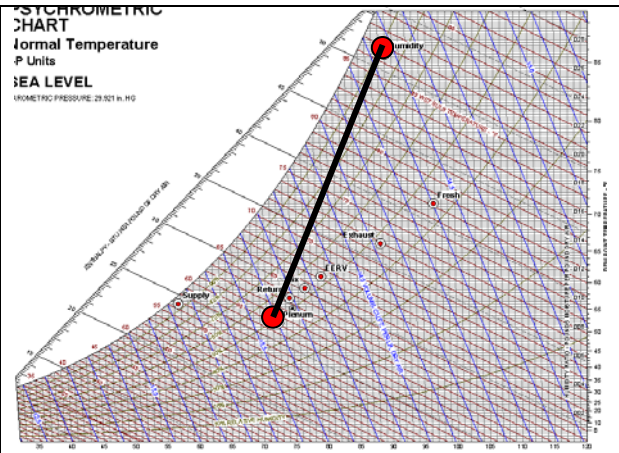


Figure 7.5. Additional facility views.

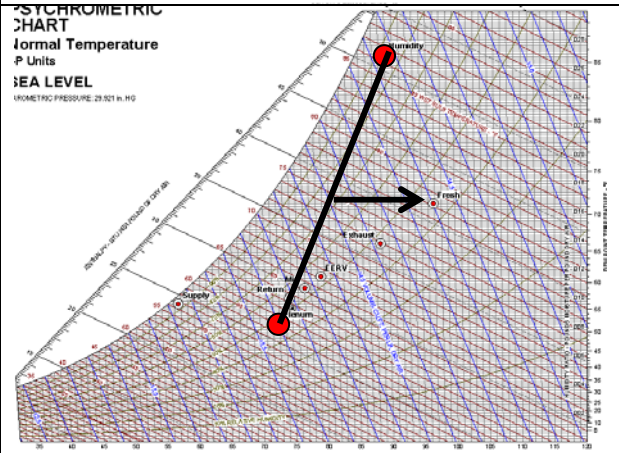
There are two plenum reservoirs from which air can be mixed to produce the return and fresh air.

1. Ceiling Plenum
2. Humidity Chamber

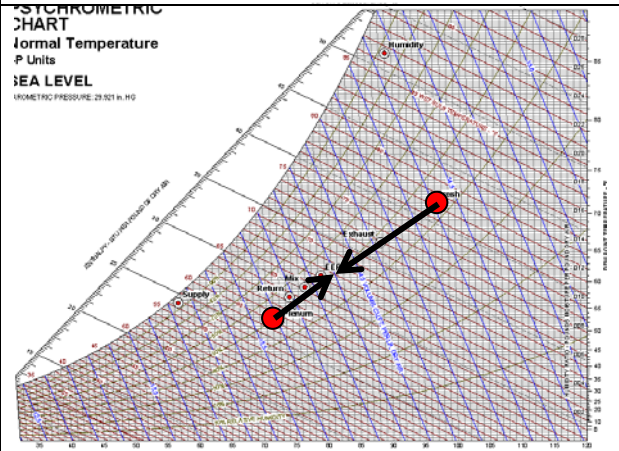
The fresh air damper-set and return air damper-set can produce any mixture between these two reservoirs.



The fresh air heater may then heat the fresh air. A closed-loop algorithm was implanted in the Carrier controller to do this task.



In bypass mode the fresh air mixes directly with the return air in the mixing plenum before passing over the coil.



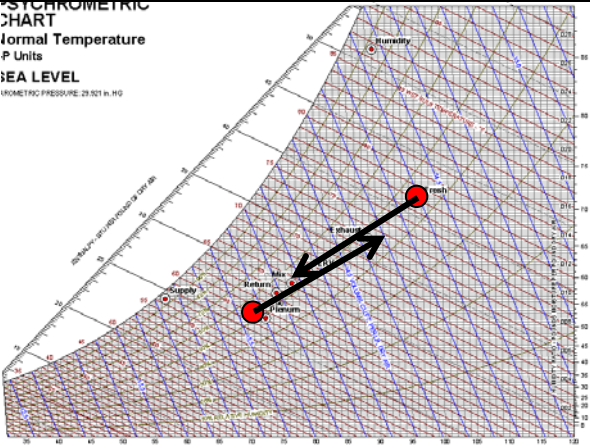
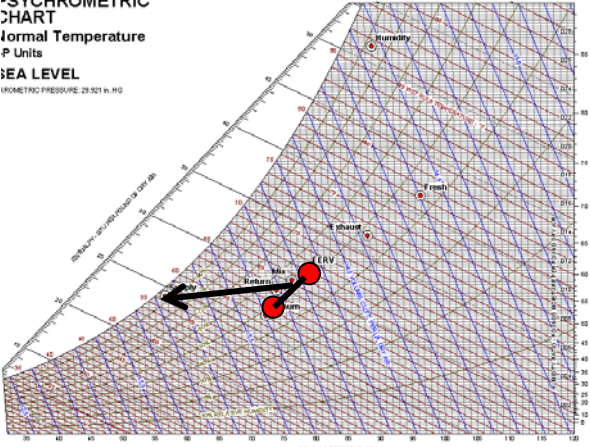


<p>In EERV mode the bypass damper is closed, and the recirculation damper is restricted to draw the fresh air through the EERV core. The exhaust fan is also turned on. The fresh air entering the mixing chamber is at a lower temperature and water content than the outdoor condition.</p>	
<p>The mixing condition is now closer to the return air condition. The mixed condition flows through the rooftop coil and is cooled. The rooftop coil can cool the supply air to a lower temperature and humidity when the EERV core is active.</p>	
<p>The supply air heater may be used to reheat the air going to the humidity zone. By controlling the humidity zone temperature the return air temperature is ultimately controlled. A closed-loop algorithm was implanted in the Carrier controller to do this task.</p>	
<p>The supply air dampers may be used to balance the air flows between the two chambers.</p>	

Figure 7.6. Facility control modes.

Data Collection and Analysis

Figure 7.7 shows a schematic diagram of the facility and instrumentation.

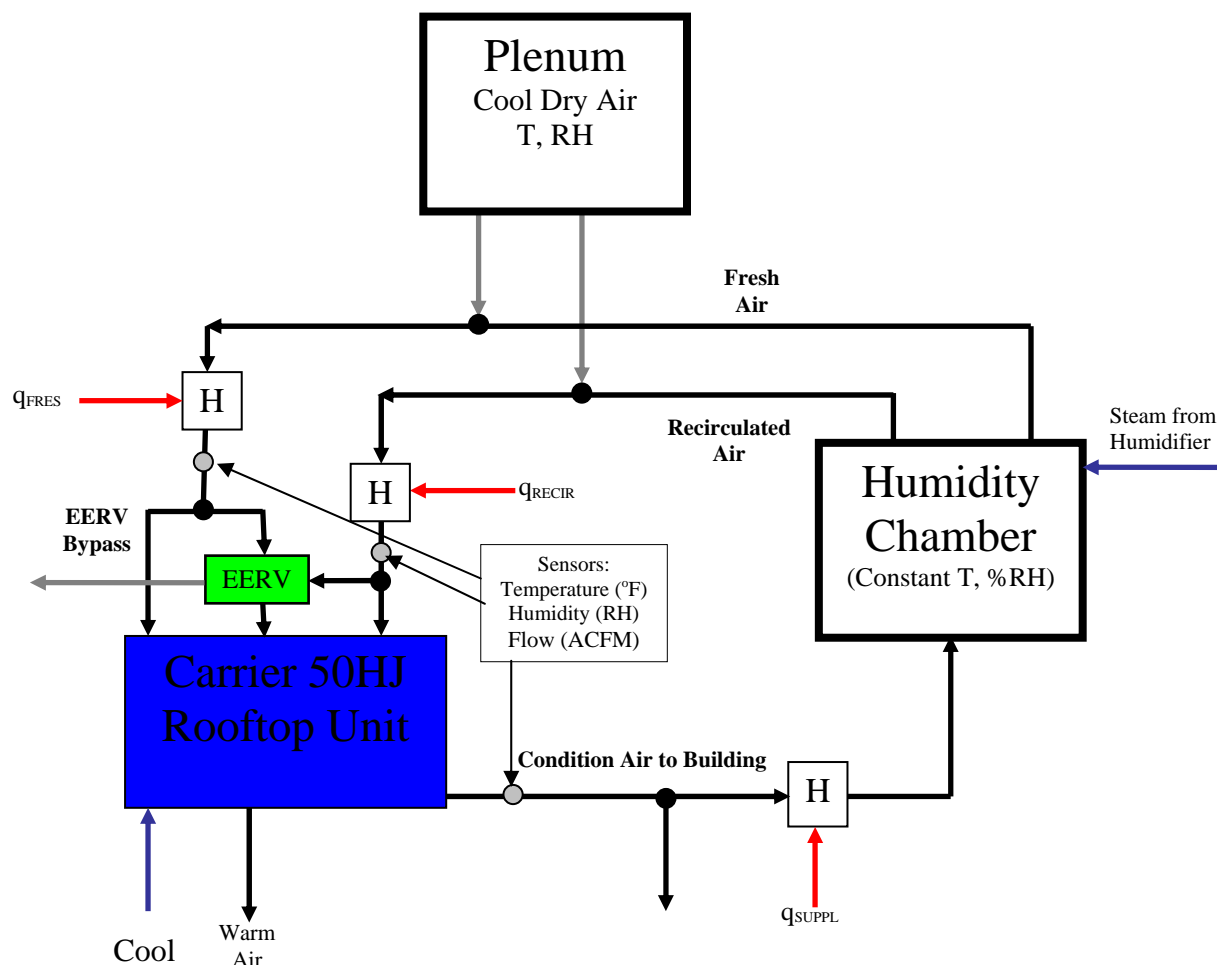


Figure 7.7. EERV test facility at UTRC.

To evaluate the performance Carrier’s 50HJ rooftop, there are two critical points that have to be measured. The first of which is the wet-bulb temperature entering the evaporator. This is calculated by determining the properties of the mixed condition resulting from combining the fresh air stream (through the EERV or the EERV bypass) with the recirculated air stream. The second point is the dry-bulb temperature of air entering the condenser. This is represented on Figure 7.7 by the “cool air” term on the bottom left. This temperature is set to be equal to the temperature of the fresh air stream. Due to the controls in place, this is not always the case. There are tests done where the dry-bulb temperature of the air going to the condenser is less than the temperature of the fresh air stream.

This variation in temperatures is taken into account when determining the system efficiency by using Carrier’s performance curves for the 50HJ and interpolating them to meet our conditions (Figure 7.8).

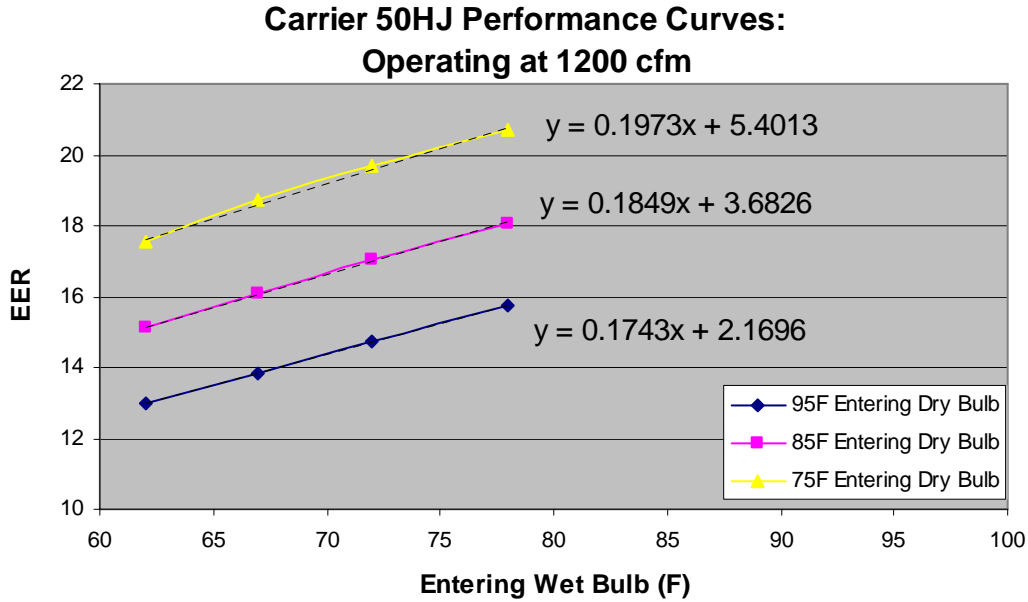


Figure 7.8. Carrier performance curves for 50HJ running at 1200 cfm.

The performance of the Carrier 50HJ rooftop and of the EERV was calculated by performing a series of enthalpy balances on the flows in UTRC's test facility (See Figure 7.7). Combining volumetric flow rates with psychrometric data for a given stream allows for the calculation of the mass flow of air. Once the mass flow of an air stream is known, the total enthalpy of that air stream can be calculated. Given the enthalpy of each air stream, the enthalpy removed by the rooftop unit and the enthalpy removed by the EERV can be calculated. The EER is then evaluated for the system according to:

$$EER = \frac{(H_{Mixing} - H_{Supply}) \cdot Q_{Mixing} \cdot \rho_{Mixing} + (H_{EERV_IN} - H_{EERV_OUT}) \cdot Q_{Fresh} \cdot \rho_{Fresh}}{Compressor_Power(W) + Fan_Power(W)}$$

where H_N is the enthalpy of stream N in btu/lb, Q_N is the volumetric flow rate of stream N in ft³/hr, ρ_N is the density of air in stream N in lb/ft³, and the Compressor Power and Fan Power represent the power draw by the rooftop.

Facility Validation

The main efforts of the evaluation experiments were focused on two primary objectives. The first was to pick a set of conditions and examine the systems ability to hold at that set of conditions. The second objective was to look at the performance of the Carrier 50HJ rooftop and determine if it is operating at Carrier's published values for capacity and power. See Table 7.4 for Carrier's performance tables.

Table 7.4. Carrier Performance Tables for UTRC's EERV Facility Rooftop

Carrier 50HJ 3-Ton Performance Specifications													
Temp of air entering the condensor Dry Bulb (°F)		900 CFM / 0.14 Bypass				1200 CFM / 0.17 Bypass				1500 CFM / 0.20 Bypass			
		Entering Wet Bulb				Entering Wet Bulb				Entering Wet Bulb			
		78	72	67	62	78	72	67	62	78	72	67	62
75	Total Capacity (1000BTU)	45.6	41.9	38.7	35.7	46.8	43.5	40.8	37.7	48.1	44.8	41.8	39
	Sensible Heat Capacity (1000BTU)	14.5	20.4	25.2	29.7	14.7	21.8	28.2	33.8	14.8	23.3	30.7	37
	Compressor Power (kW)	2.24	2.19	2.16	2.12	2.26	2.21	2.18	2.15	2.28	2.23	2.19	2.16
85	Total Capacity (1000BTU)	44.4	40.7	37.5	34.5	45.7	42.1	39.3	36.4	47	43.5	40.4	37.6
	Sensible Heat Capacity (1000BTU)	14.1	19.9	24.7	29.2	14.4	21.5	27.7	33.2	14.8	23.3	30.3	36.4
	Compressor Power (kW)	2.51	2.46	2.42	2.39	2.53	2.47	2.44	2.41	2.54	2.5	2.45	2.42
95	Total Capacity (1000BTU)	42.9	39.3	36.1	33.1	44.6	40.8	37.8	34.9		42	38.9	36.1
	Sensible Heat Capacity (1000BTU)	13.6	19.5	24.1	28.4	14	21.1	27.2	32.5		22.8	29.9	35.6
	Compressor Power (kW)	2.8	2.75	2.71	2.66	2.83	2.77	2.73	2.69		2.79	2.74	2.71
105	Total Capacity (1000BTU)	41.3	37.7	34.6	31.7		39.3	36.2	33.4		40.1	37.2	34.7
	Sensible Heat Capacity (1000BTU)	13	18.8	23.5	27.8		20.7	26.6	31.8		21.3	28.7	33.2
	Compressor Power (kW)	3.11	3.06	3.02	2.98		3.09	3.04	3.01		3.44	3.41	3.37

UTRC decided to use the ARI conditions for fresh air, at 95°F and 47.3% relative humidity, and return air, at 75°F and 51.6% relative humidity. UTRC's controls were able to hold the system stable around the set point. See Figure 7.9 for the psychrometric chart of the validation data. Other conditions that were tested are discussed below.

In order to reduce the oscillations in the humidity chamber, UTRC engineers made modifications to the humidifier so that it will run a "fast refill and reheat." Also a tankless water heater was installed upstream of the humidifier to preheat the water to 150°F before it enters the humidifier. The modifications allow reduce the oscillations to acceptable levels, less than +/- 5% relative humidity.

The system was delivering 1230 cubic feet per minute, 5575 lbs of dry air per hour, of conditioned air, at 47% outside air fraction. The rooftop unit was delivering 3.5 tons of cooling and had an EER of 15.9. At these conditions, the Carrier 50HJ is reported to have an EER of 14.8. The variation between experimental and literature values is approximately 7%.

EERV Performance

In order to ensure experimental consistency, the systems performance is measured in EERV mode and non-EERV mode in back to back tests. This procedure allows for the test conditions, temperature and humidity, to be duplicated as closely as possible for the EERV mode and non-EERV mode. One of the reasons for this is due to the conditions of the plenum, the reservoir for cool dry air (Figure 7.7), which are not controllable and may vary slightly from day to day.

With the EERV inserted in the system, at ARI conditions, the sensible and latent recovery factors observed were 0.78 and 0.67 respectively. This is in agreement with the BP1 results obtained at Intertek/ETL and NREL, within the experimental error of the test facility. The EERV was measured as recovering 0.9 tons at about 500 cfm and 33% outside air fraction.

After the completion of the validation experiments, the integrated system was tested in a range of conditions. A sample of the data is listed in Table 7.5 below. A psychrometric chart of the normal operating range of the integrated system is shown in Figure 7.10.

Validation Run – System Holding at
ARI Conditions.

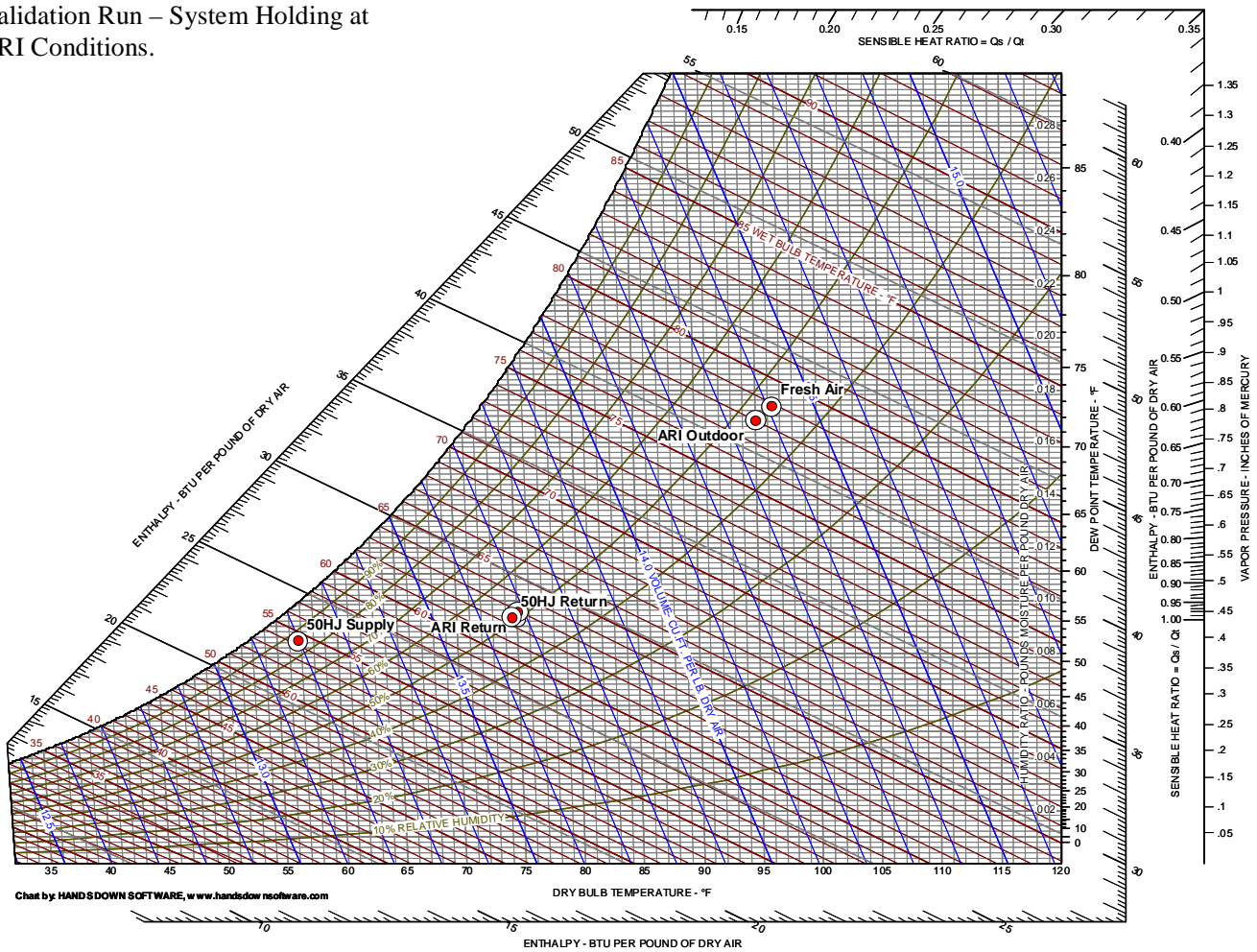


Figure 7.9. Psychrometric chart during a validation run.

Table 7.5 Sample of Data Collected in EERV Mode

Dry-bulb Entering Condenser (°F)	Wet-bulb Entering Coil (°F)	% O.A.	Outside Air Flow cfm	Tons Cooling	Effective EER	Sensible Effectiveness	Latent Effectiveness
89	66.4	43%	484	4.34	17.3	0.61	0.59
82	66.1	33%	389	4.03	17.5	0.78	0.67
95	64.9	33%	414	3.60	14.1	0.92	0.77
95	62.7	43%	452	3.56	14.2	0.74	0.73
95	67.1	38%	424	3.92	14.8	0.79	0.75

Different modes run with EERV system. This data shows the area where the system has been operating most frequently
S = Supply Air
R = Recirculated Air
F = Fresh Air

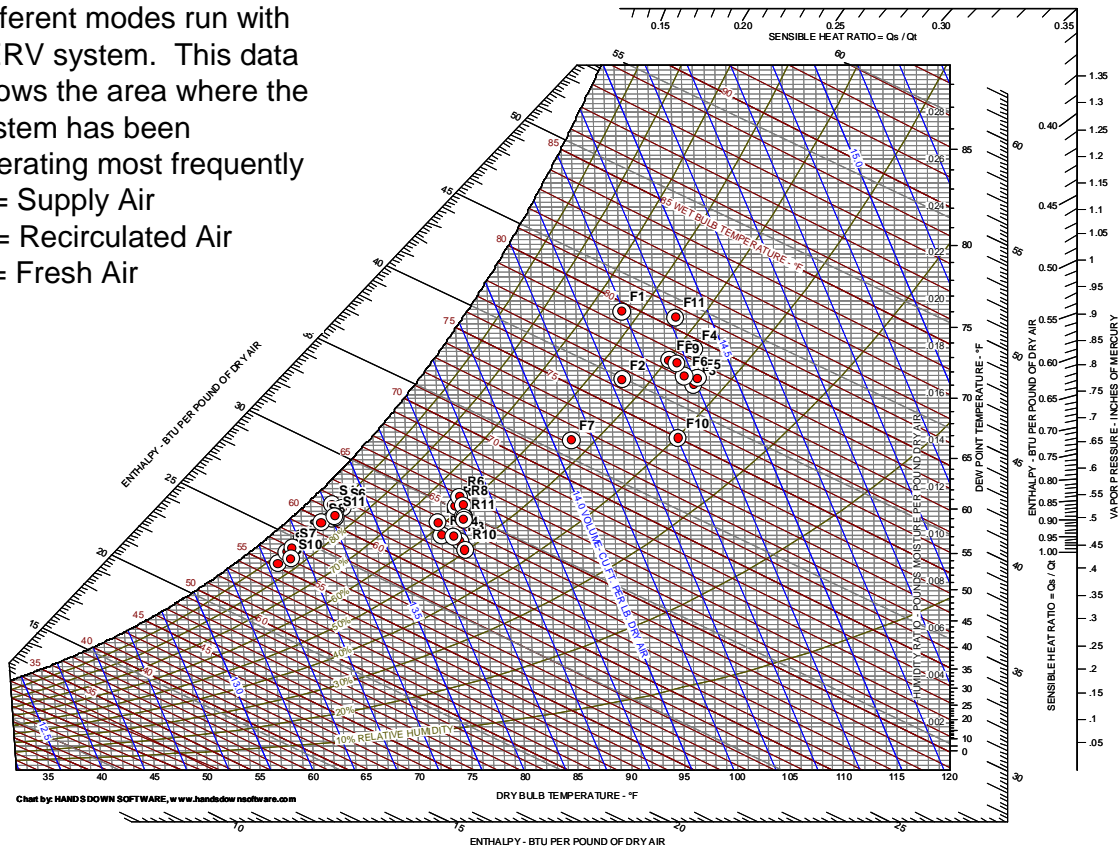


Figure 7.10. Normal operating conditions of integrated system.

Table 7.6 Sample of Data Collected in Non-EERV Mode

Dry-bulb Entering Condenser (°F)	Wet-bulb Entering Coil (°F)	% O.A.	Outside Air Flow cfm	Tons Cooling	Effective EER
90	72.0	47%	600	3.74	14.8
82	67.4	34%	400	3.16	13.6
81	70.3	34%	445	3.72	15.9
97	70.5	38%	490	3.41	13.3
96	68.5	41%	450	3.34	13.3
96	72.6	47%	525	3.74	14.1

In EERV mode, the average increase in the integrated system's EER is 11% over non-EERV mode being run at similar conditions. The average heat removed by the EERV is 1.2 tons. The average sensible and latent effectiveness' are 0.77 and 0.70 respectively.

The impact of the EERV on the system is best illustrated by looking at the difference in the mixing conditions reaching the evaporator. The less energy the rooftop has to remove, the more

efficient the overall system will be. The removal of approximately a ton of sensible and latent heat results in an average drop of 5 btu per pound of dry air. This effect can be seen in Figure 7.11.

Controls Development and Implementation

The goal of this task was to not only provide the demonstrator with a simple control system that was adequate for running performance tests, but to create the foundation for the control system that might actually be the basis for the controls used in an eventual commercialized product. As such it was desirable to use the platform already built into the exiting rooftop unit and modify it as necessary. Since (1) the existing unit was a Carrier Comfort Network (CCN) based system, (2) CCN is also still the prevalent system on new unitary products from Carrier, and (3) exiting controls software code was available that could be incrementally modified for this task, CCN was chosen for this project.

In this stage of controls development it is assumed that the EERV is either active (exhaust fan on and fresh air forced through the core) or inactive (exhaust fan off and fresh air bypasses the core). It may be that future analysis will determine an efficiency or comfort benefit to partial operation (variable speed exhaust fan and modulating bypass damper or variable speed boost fan). In that case, a cost/benefit analysis will be performed to determine if the added benefit is worth the added component costs. With the active/inactive only deployment there are three primary modes of rooftop/EERV operation:

- Heating and Cooling without economizer: The outside air always produces a load in commercial heating modes. In cooling mode the economizer logic makes the decision as to whether the outdoor air can produce beneficial cooling and/or dehumidification. If not, then the unit runs in cooling mode. Since the outside air load is not desirable full EERV recovery is used.
- Cooling with Economizer: The decision has been made that the outside air is beneficial to providing cooling. Recovery is not desired. The EERV is deactivated.
- Band between economizer and cooling: If the outside air represents only a small load, it is possible that it is more efficient to turn off the EERV and bypass the fresh air than to pay for the extra fan power.

Table 7.7 shows the EERV related actuators during the three modes described above.

Table 7.7 EERV Actuators

Mode	Boost Fan or	Recirc Damper	Exhaust fan	Bypass damper
Heating or Cooling	On, DP = 0.5"	Restricted, DP = 0.3"	On, DP = (0.5+0.2)"	Closed
Economizer	Off	Open	On or off	Modulating
No EERV	Off	Open	Off	Closed.

The pressure drops shown in Table 7.7 are based on –0.2 inches of water pressure normally in the mixing chamber and 0.5 inches through the core. The recirculation damper must add 0.3 inches of pressure drop.

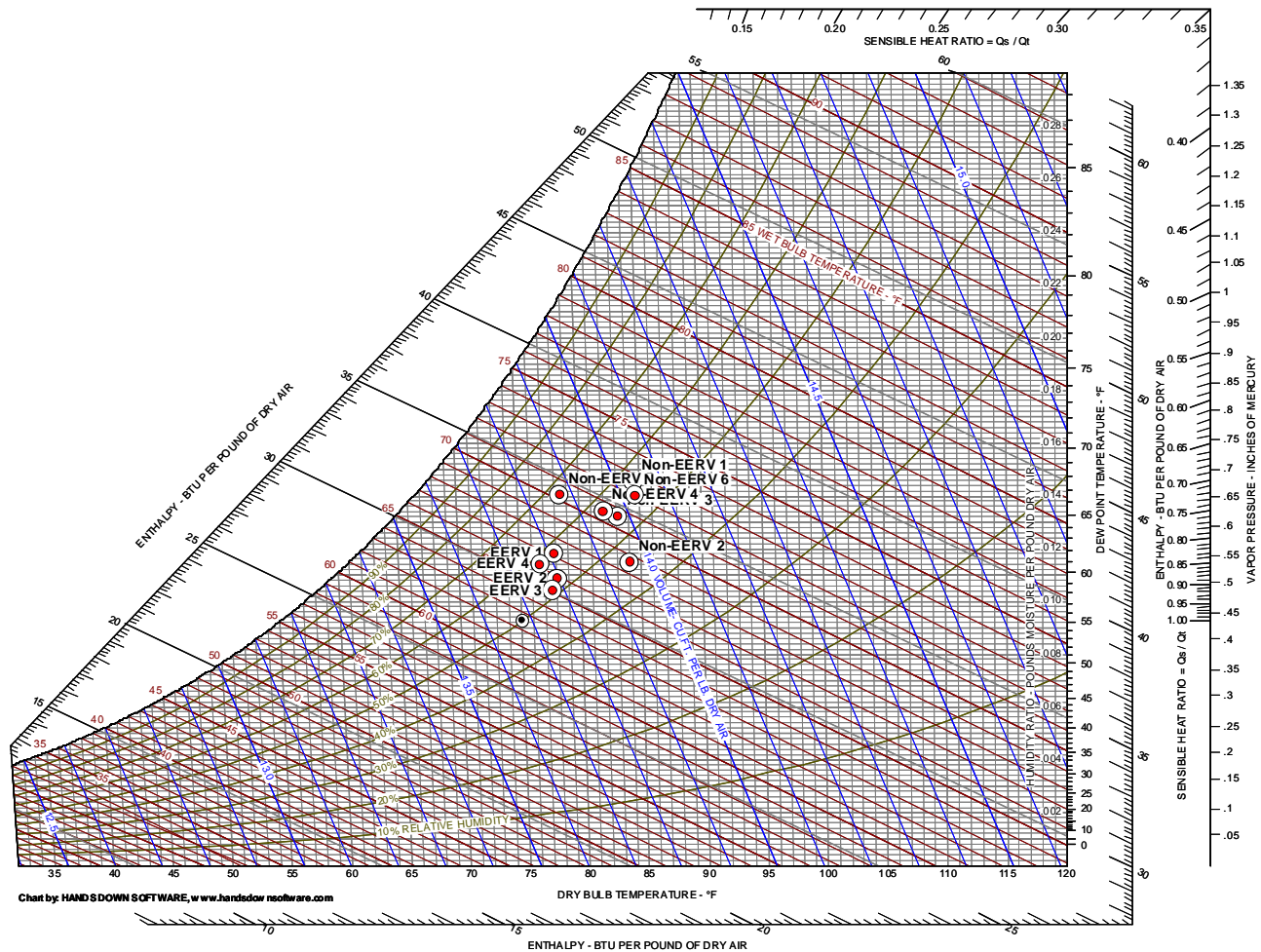


Figure 7.11. Mixing conditions in EERV mode and non-EERV mode.

Determining the Need for EERV Bypass In Cooling Mode

It is important to note that the extra fan power associated with running the EERV need not be realized unless there is a net gain in system efficiency. The proposed EERV/rooftop system can remove all fan penalties by simply bypassing the fresh air around the EERV core. The exhaust fan is turned off, and either the boost fan is turned off or the recirculation damper is opened to remove any unnecessary pressure drop. The control logic continuously determines whether to use the EERV during cooling mode.

Break-even occurs when the enthalpy load of the fresh air is equal to the exhaust fan power plus 2 times the supply or boost fan power. (The supply or boost fan heat add to the sensible building load.)

Table 7.8 Sample Fan Power Calculation

	Exhaust Fan	Boost Fan	Supply Fan
cfm	360	360	1200
DelP (in H ₂ O)	0.7	0.5	0.3*
Flow Power (W)	29.6	21.2	42.3
Fan eff.	0.3	0.3	0.5
Electr. Power (W)	98.7	70.5	84.6

* Delta increase in pressure required for EERV operation.

For the example above, the enthalpy difference between the fresh and return air at break-even (for damper method) can be determined from the following equations:

$$\text{Total Power Damper method} = 98.7 + 2 \times 84.6 = 268 \text{ w.}$$

$$\text{Power expressed in btuhr: } 268 \text{ W} = 914 \text{ btu/hr.}$$

$$\text{Mass flow of fresh air} = 360 \text{ ft}^3/\text{m} \times (0.074 \text{ lbm}/\text{ft}^3) \times (60 \text{ m/hr}) = 1600 \text{ lbm/hr.}$$

$$\text{DH} \times \text{mdot}_{\text{air}} = \text{Electric Power}$$

$$\text{DH} = 914 \text{ btu/hr} / (1600 \text{ lbm/hr}) = 0.57 \text{ btu/lbm.}$$

This corresponds to about 2 degrees F of sensible load.

Frost and Condensation Control.

An EERV or enthalpy wheel is less susceptible to frost than a standard sensible only method of recovery. Figure 7.12 shows two operating conditions for the EERV, and one (red dashed line) for a sensible only method.

- During a damp cool day (red circle) the fresh air is dried and the exhaust air becomes more humid but does not reach 100% RH.
- During a cold day (blue circle) the exhaust stream of a sensible recovery device may saturate and freeze. The EERV is shown with approximately equal latent and sensible effectiveness. Condensation and frost is avoided.

Figure 7.13 shows operation at high indoor humidity and low outside temperature. It is possible under these abnormal conditions that condensation and frost will occur somewhere in the core. Since the core is cross-flow, the local conditions at various locations through the core are both more and less extreme than the average shown in the plot. The control system must recognize conditions that will lead to condensation and/or frost, and avoid operation during these conditions. If frost should occur it can be removed by running the exhaust fan while the fresh air is bypassed. This will heat the entire core to the return air condition.

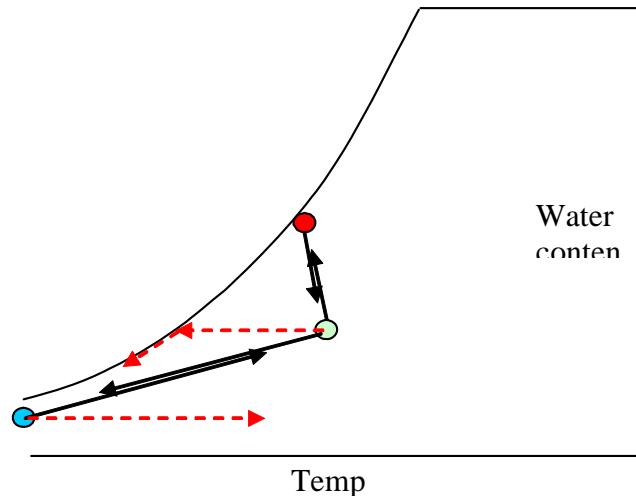


Figure 7.12. Operation with humid outdoor conditions.

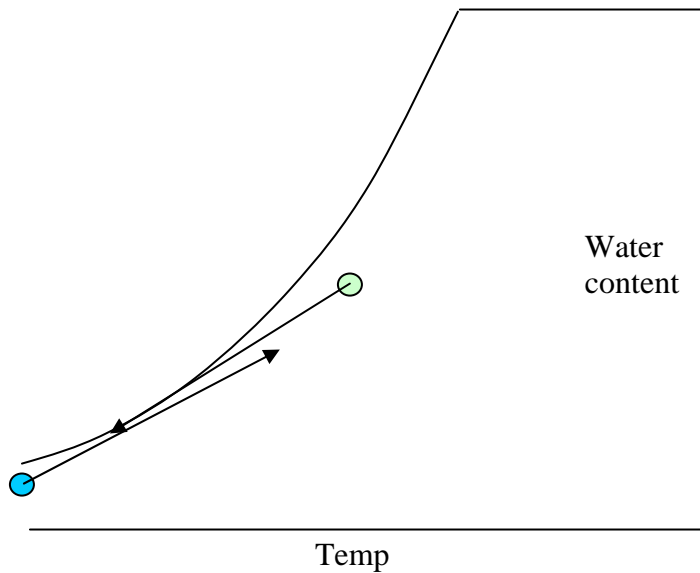


Figure 7.13. Operation with humid indoor and outdoor conditions.

Laboratory Measurements

The BP2 data collected was examined at the start of BP3 and it was found that there were a few gaps in the dataset. These were judged to be important enough to warrant some additional testing. The two classes of conditions identified for which data is needed for design decisions are (1) relatively cool but humid (part load) conditions that require a low coil sensible heat ratio, and (2) operation near the cooling design day conditions at higher air flow rates. There is also the continuing objective of repeating a standard run to see if accumulated run time has had any effect on membrane performance.

Experiments were conducted to simulate low outside air temperatures with high humidity conditions. The target conditions for the system were:

- Fresh air stream: 75 F DB and 75% RH,

- Return Air Stream: 75 F DB and 50% RH.

Table 7.10 Reproducibility Run Results

RUN	EERV	Outside Air Temperature	Outside Air Relative Humidity	Outside Air Flow	Energy Recovered by EERV	Total Cooling	System EER	Sensible Effectiveness	Latent Effectiveness
	On/Off	°F	%	acfm	tons	tons	-	-	-
Check Run	Off	95	48%	475	-	3.2	12.3	-	-
Check Run	On	95	48%	480	1.5	3.64	13.2	0.81	0.72

To setup for the final condition in the run series, the 50HJ Weathermaster was modified to run at a higher flow rate (face velocities in excess of 200 ft/min or 600cfm) with the intention of measuring the performance of the EERV with higher outside airflows. A new exhaust fan was installed. The fresh stream was maintained at 95°F and approximately 40% RH and the recirculated air was maintained at 75°F and approximately 45% RH for the tests. The supply and exhaust legs of the EERV were analyzed to determine the sensible and latent effectiveness. The amount of water transferred across the membrane was calculated for each stream in order to make sure the mass balance was closed. The mass balance for the high flow runs did not close as well as it did for low flow runs. Table 7.11 below represents one high flow run. The sensible effectiveness agrees quite well comparing the value based on inlet vs. exhaust measurements. There is more of a problem in the water mass balance and, consequently, the latent effectiveness. The supply side value more than exceeds the requirement of ASHRAE 90.1. The exhaust side value is probably too high, as the latent effectiveness is typically lower than the sensible. On the other hand, the average value of 0.68 is close to expectation.

Table 7.11 High Face Velocity Run

	Supply Side	Exhaust Side	Error
<i>H₂O Transfer (lb/hr)</i>	11.62	7.32	32%
<i>ε_{SENSIBLE}</i>	0.75	0.74	1%
<i>ε_{LATENT}</i>	0.53	0.83	32%

During a typical run, the humidifier that supplies steam to the humidity source refills approximately eight times every hour. Each time a refill cycle begins, it causes a drop in the humidity throughout the system. Tests were conducted to explore the impact of the humidifier refilling on the sensible and latent effectiveness.

There was no measurable impact of the humidifier refilling on the sensible effectiveness. There was an approximately 5% deviation in the latent effectiveness due to the humidifier refilling. Figure 7.15 illustrates an extreme in the differences observed between the sensible and latent effectiveness for a high flow run. The perturbations in the chart represent the humidifier refilling.

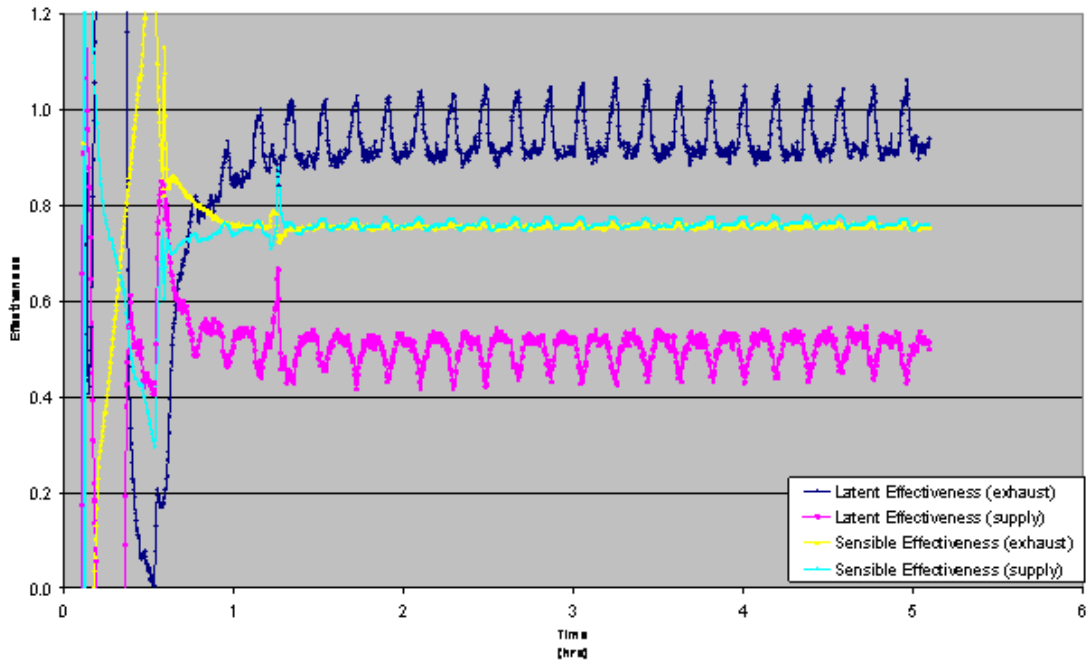


Figure 7.15. Transients during high-flow run.

Optimized Demonstrator Configuration

In the design of the optimized system one general theme that has evolved is to adjust flow with variable speed motors as more practicable rather than using dampers. This will permit the economizer of the unit to be restored to its original design. At times when the sensible energy expended to overcome the EERV pressure drop would exceed the energy recovered, the economizer will be cracked open to bypass the EERV and the EERV fans will be shut off. While a dedicated outside air fan is less efficient than the system fan, the former runs continuously and the latter runs only when cooling is needed. Current thinking is that it makes more sense to run the dedicated outside air fan and move the smaller amount of air. A dedicated exhaust fan will help attain mass flow balanced operation.

A psychrometric spreadsheet was developed that includes the design conditions for all US cities for which EnergyPlus data is available. Using this spreadsheet it is possible to calculate the optimal sensible heat ratio (SHR) of a cooling coil with and without an ERV present. Most unitary DX coils are sold with a SHR around 0.7. This analysis shows that the SHR should be higher when an ERV is incorporated. Figure 7.16 shows the effect for the Miami design day. Instead of selecting a thinner coil, the face velocity of the air moving through the coil can be changed to modify the instantaneous SHR. A variable speed supply fan will permit this type of control.

Finally, one of the reasons that unitary equipment does not ordinarily provide fine humidity control is that at the end of each cooling cycle the outside air fan continues to run. If this air travels through the mixing plenum and coil, water condensed on the coil can be re-evaporated into the air stream. When an EERV is present the preconditioned outside air will be partially conditioned by the exhaust air (even though the compressor is off). If this air is inserted downstream of the coil, the coil will not be warmed by outside air passing through it when cooling is not required and it will remain cooler between cycles. This will not only eliminate the

re-evaporation phenomenon at the cycle's end, but also mitigate the effect that occurs at the beginning of each cycle wherein as the refrigerant starts flowing it takes several minutes for the coil exit temperature to drop below the dew point and begin to condense water. Until that time there is sensible cooling but no dehumidification. Geometries for inserting the makeup air downstream of the coil were also investigated.

To test the degree to which it would be advantageous to insert this air downstream of the coil a design was developed that will have a manual shunt that will permit back-to-back comparison of injecting this air upstream and downstream of the coil.

In summary, the new design for the integrated EERV/rooftop embodies the following major changes from the prior demonstrator:

The previous design used part of the economizer damper to generate a pressure drop into the mixing-box. Fresh air was pulled through the economizer by the negative pressure (typically – 0.5 in.-wg). The new method uses a boost fan.

The previous design had modified the economizer and had placed the EERV core adjacent to the economizer dampers. The EERV assembly is now mounted on the top of the rooftop unit, and the economizer is not modified.

The exhaust and blower fans will be electrically commutated DC motors (ECM) that can be programmed with the specific blower characteristics so that they can control to cfm. These motors automatically adjust for varying system pressure drops. They can also be used for diagnostics.

The primary supply blower of the rooftop will also be changed to an ECM blower. This will allow reduced fan power draw when only ventilation air is required.

Provisions will be made so that the conditioned fresh air from the economizer can either be sent to the mixing-box (normal) or directly into the supply duct. The goal is to be able to stop or minimize the flow of air over the coil when the unit cycles off in cooling mode. This will prevent re-evaporation of the condensed water and improve humidity control.

Figure 7.17 is a schematic of the integrated design to be tested in the UTRC laboratory. Different duct and fan orientation may be required for an actual product.

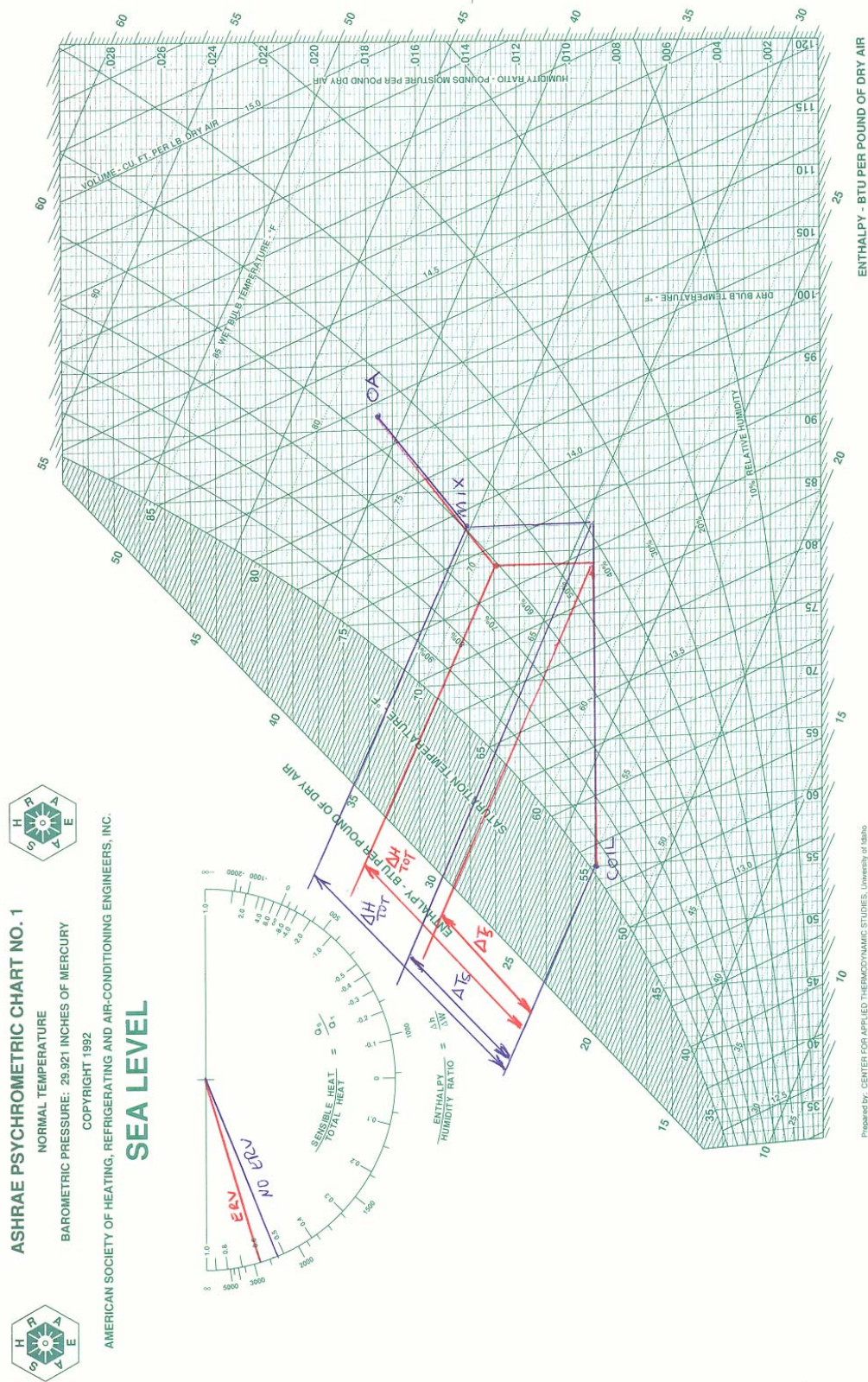


Figure 7.16. Psychrometric paths with and without an ERV preprocessor.

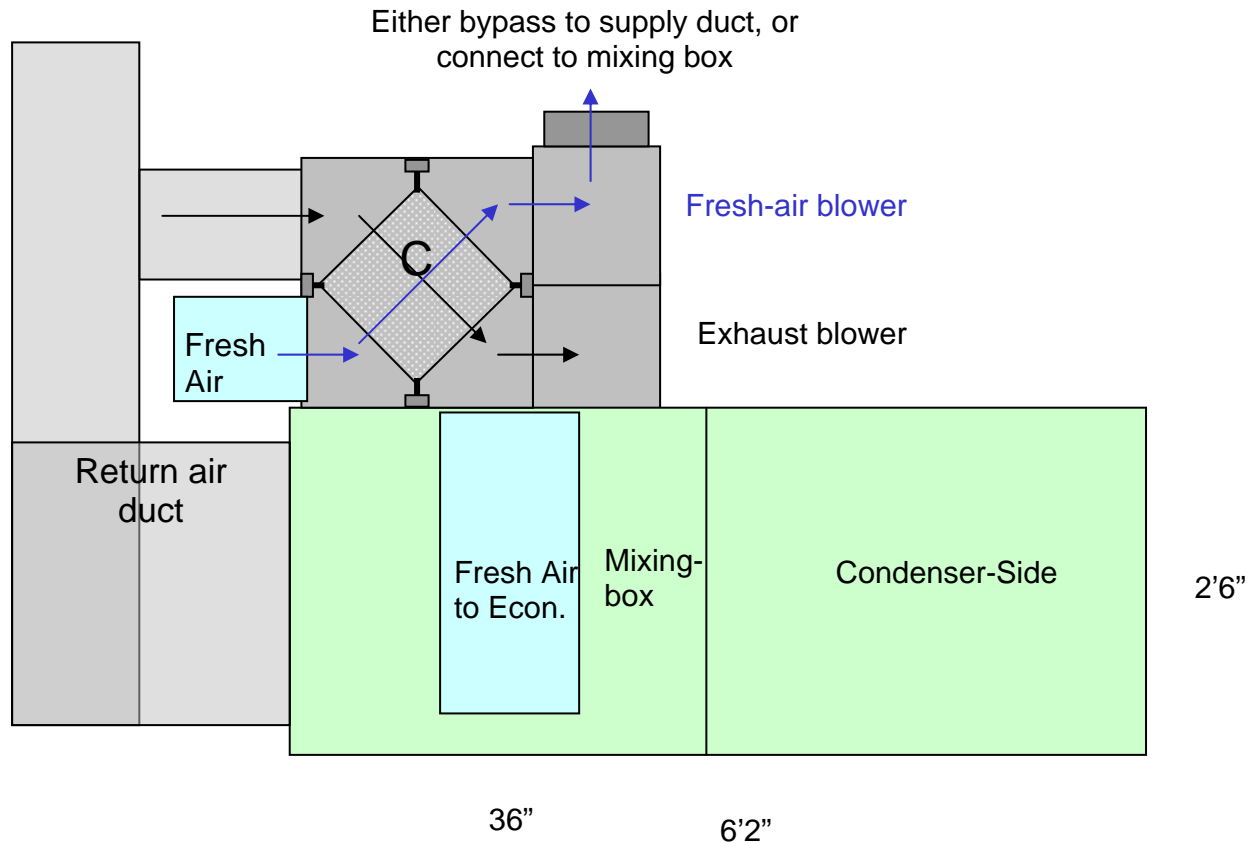


Figure 7.17. Optimized integrated EERV/Rooftop unit. Front view on return and mixing-box side with fresh air flow (blue) visible into mixing box.

The plastic enclosure for the EERV is shown in Fig. 7.18, and the finalized optimized system in Figs. 7.19-20.

Variable Speed Fans and Controls

Figure 7.21 shows that the new configuration uses three variable speed fans: (1) main supply fan, (2) fresh air boost fan, and (3) exhaust fan. This was considered a better configuration than the BP2 configuration that operated the supply fan when conditioning is not required.

The main supply fan is still the standard blower that came with the 50HJ004 rooftop unit from Carrier, but it is now being driven by a 1.5 HP ABB inverter. The motor was changed from single to 3-phase. The fresh-air and exhaust fans are backward curved “plenum” fans provided by EBMPapst, model number R3G280. These fans are integrated units which include a DC motor and the necessary ECM power electronics. The speed of each of the three fans is now controlled via analog control signals from the Carrier CC6400 control modules.



Figure 7.18. EERV core in custom Plexiglas® manifold. Protective paper has not yet been removed.

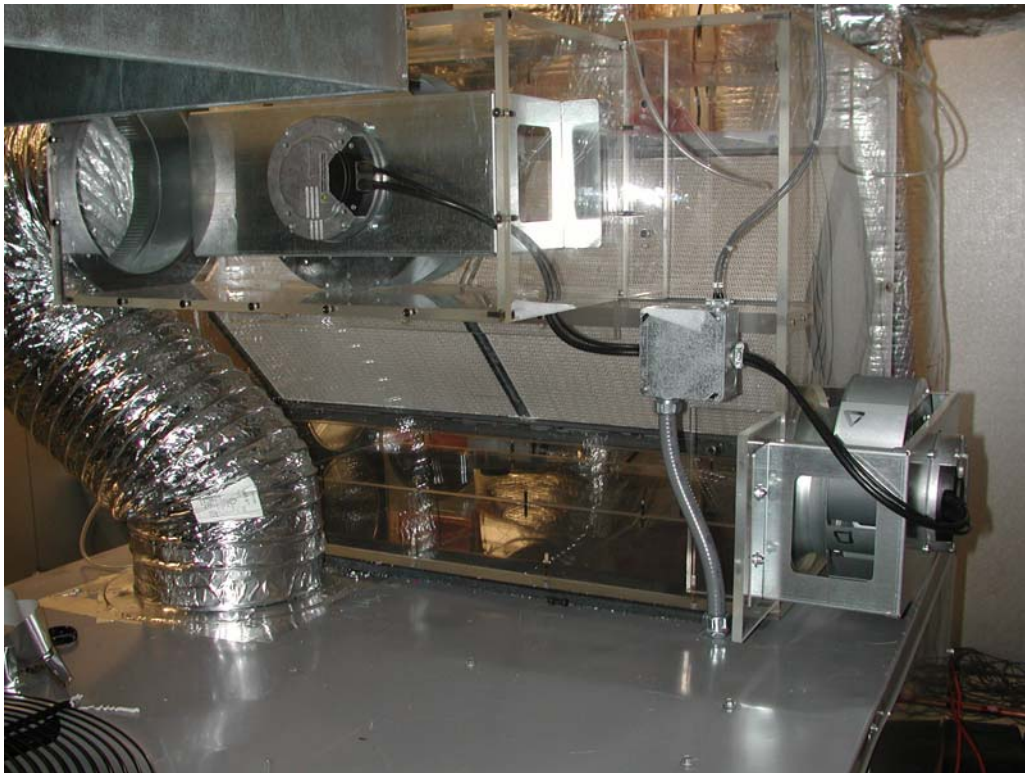


Figure 7.19. Close up view of the horizontally-oriented EERV core attached across the top of the rooftop.



Figure 7.20. View of the completed integrated EERV/rooftop unit.

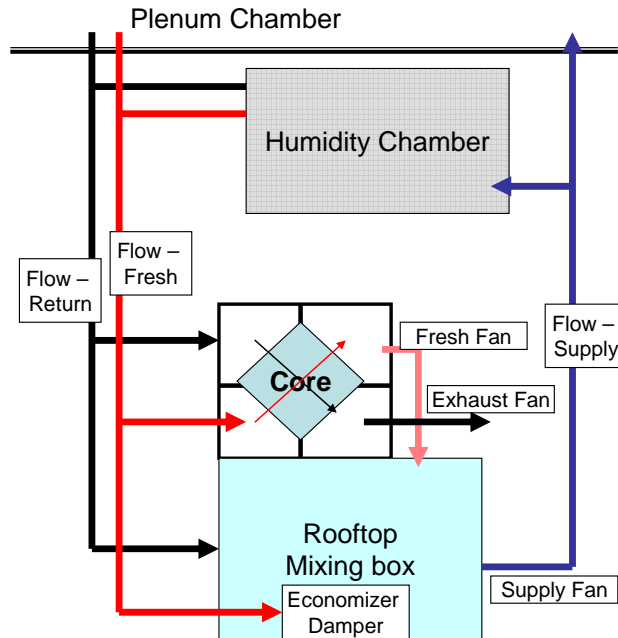


Figure 7.21. Schematic of new configuration showing fan locations and flow measurement stations.

Speed control of Fresh-air and Exhaust fan

The fresh-air and exhaust fans are powered by single-phase 208 or 230 V. They are controlled by a 0-10 V analog signal. The rotational speed of each fan was measured for a variety of control signals and operating pressure differential, and was checked for repeatability.

The speed response was found to be linear from about 2.5 V (800 rpm) to 8 V (2600 rpm). For our application the nominal speed is approximately 1000 rpm to 1700 rpm, which is within the linear range.

Calibration of the velocity (air-flow) meters.

In order to calculate an energy balance for the rooftop system, air velocity probes by Volu-probe and differential pressure transducers by Veltron have been installed in each of the three main ducts: Supply, Return, and Fresh Air. The Veltron transducer has a precision of one-thousandths of an inch of water. With the variable speed fans it is now possible to slowly vary the air volume pulled through each of these ducts. The location of the flow measurement stations is shown in Fig. 7.21. The supply fan is used to vary the flow through the return and supply ducts, while the fresh-air fan is used to vary the flow through the fresh-air duct. For these tests, the plenum openings were closed so that all of the air that passes the flow station must also flow into or out of the humidity chamber. Air-leaks that occur at the core or rooftop unit do not affect these calibrations. The flow at the humidity chamber was measured with a flow hood. The measured flows agreed well with the calculated flows based on the dynamic pressure as measured with the flow probes.

Pressure drop through the core

Data is available on the vendor website for a similar but smaller core. This core is a 10 ¾" cube. Pressure drop is shown to be linear for up to 140 cfm for this core. The core we are testing is

12" x 12" x 39" wide. A first-order approximation predicts that pressure drop is proportional to width divided by volumetric flow. For laminar flow the pressure drop increases with length and decreases with velocity. Increasing the height decreases the velocity. Therefore, increasing the length and height proportionally should not change the pressure drop. Figure 7.22 shows a test where the exhaust fan was used to pull air through the core.

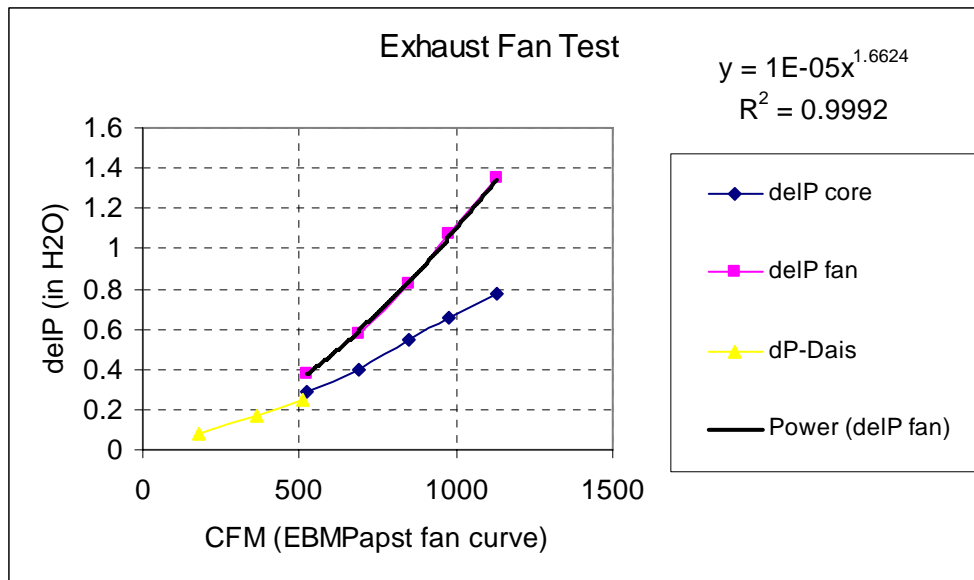


Figure 7.22. Exhaust fan performance and core pressure drop.

The scaled vendor data is shown in yellow. Our measured core pressure drop is in blue, and the full fan pressure rise is magenta. From this test it can be noted that:

- at our nominal flow rates of 300 to 600 cfm the core pressure drop is less than 0.5 in w.c..
- the measured core pressure drop is consistent with vendor data.

Also during this test the fresh-air fan was turned to a high flow rate to determine if there would be any affect on the exhaust side of the core. There was no noticeable effect. This indicates that

- core leakage is not significant, and
- core billowing (that would change the pressure drop for a given flow rate) is not significant.

Control with variable speed blowers

The optimized system allows a greater degree of control over individual parameters contributing to the conditions of each flow, but individual control parameters can influence more than a single stream. With three individually controlled fans on the supply, fresh and exhaust flow paths, a greater degree of control is available in the optimized system over the previous means of using dampers alone to control the same flows. However, there is interaction between the eight dampers and three fans in that the pressures developed at various points in the system through individual damper and fan settings influence the final flows in each duct.

This introduces a somewhat larger than expected complexity in the controls for the device and its interaction with the controls for the facility in which it is being tested. In any case, tuning the facility to achieve the required conditions could be done. This is somewhat exacerbated by the fact that in the “shoulder season” for HVAC there is great variability from day to day outdoors

and the internal airflows the facility draws on from the building are not quite independent of the outdoor ambient conditions.

Carrier uses ECM motors that are programmed so that they can accept a cfm command from the unit controller. They internally vary their speed to achieve the desired cfm. The ECM fan controllers that do this are programmed with the fan/blower characteristic curves:

$$\text{Power} = f(\text{speed}, \text{volume flow})$$

$$\text{delP} = f(\text{speed}, \text{volume flow})$$

Speed is known since permanent magnet motors are synchronous with the electrical switching. Power is also known by the drive. The ECM controller can calculate the volumetric flow from the power curves, and the pressure rise from the flow curves.

Reprogramming the blowers used for the BP3 demonstration was beyond the scope of this project. The required blower speeds were estimated from the laboratory instrumentation, and were commanded directly from the Carrier CC6400 controllers.

Control of the Fresh-air Boost Fan and Economizer

Fresh air can enter the mixing plenum either through the EERV or directly through the economizer opening. The economizer used for BP3 is the standard unmodified horizontal option sold by Carrier. It consists of two dampers driven by a single stepper motor (Fig. 7.23).

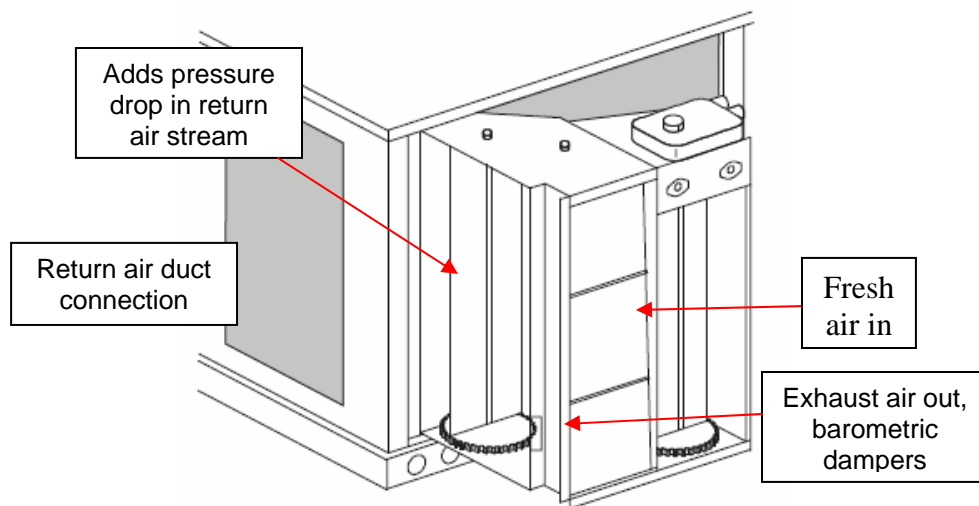


Figure 7.23. Economizer positioned for installation into the rooftop unit.

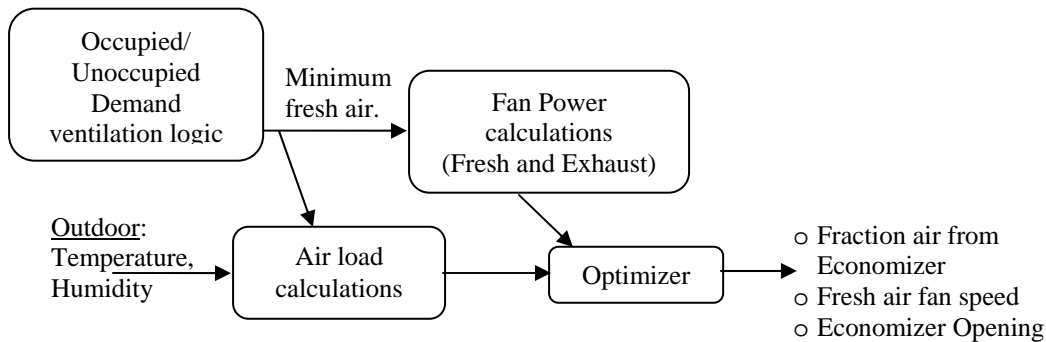
One damper connects the mixing plenum to the outside air; the other adds a pressure drop to the air returning from the building to the plenum. When the economizer is at 0% open, the outside air damper is closed and the other is at minimum resistance. When an economizer is used without an EERV, to achieve the required ventilation rate, it is set to a minimum opening (default = 20%) and never closes during operation. It may then open further during economizer mode (roughly determined as the outside air having less enthalpy than the return air). When an economizer is used with a recovery ventilator it is set to 0% during non-economized operation.

Since the mixing box operates at a pressure below atmospheric, some fresh air will flow through the EERV core even without the fresh-air fan running. The fresh air fan is used to boost the

fresh air flow to the desired level. The fresh-air fan does not need to run as fast as the exhaust fan, nor consume as much power, for a given flow rate.

Three modes of cooling operation can be defined with the EERV and economizer:

1. Fully economized: The outside air is better (lower enthalpy) than the return. The exhaust and boost fans are turned off. The economizer is opened to help condition the supply air.
2. Fully EERV: The energy recovered by the EERV is greater than the extra fan power expended. The economizer is closed. The fans are operated to achieve the desired fresh air flow rate.
3. Band in between: The fan speeds and the economizer opening are varied to maintain the desired fresh air flow rate and minimize the total load due to ventilation.



Fan power is proportional to cfm raised to a power between the 2 and 3. Because of this non-linear effect, it may be optimum to run the fan at part speed providing some of the fresh air from the EERV and some from the economizer. The details of this trade off will be specific to the final product specifications.

An example of this optimization is presented below. The following assumptions are made:

- o Desired Fresh air flow rate: 400 cfm
- o Fan (boost and exhaust) power at full flow: a) 150 W; b) 300 W
- o Fan power proportional to the flow raised to the 2.5 power.
- o Recovery efficiency: 80% (constant)

In Figure 7.24,

- o X-axis: flow through core varied from 0 to full (400 cfm), remainder through economizer.
- o Y-axis: total building load due to ventilation load (w) = fan power + enthalpy load of air coming through the economizer + enthalpy load of air coming through the EERV.
- o Lines on each plot: Air enthalpy load varied from 1 to 6 degree F equivalent sensible load. (1 degree sensible load produces 0.24 btu/# times the flow rate in #/hr).

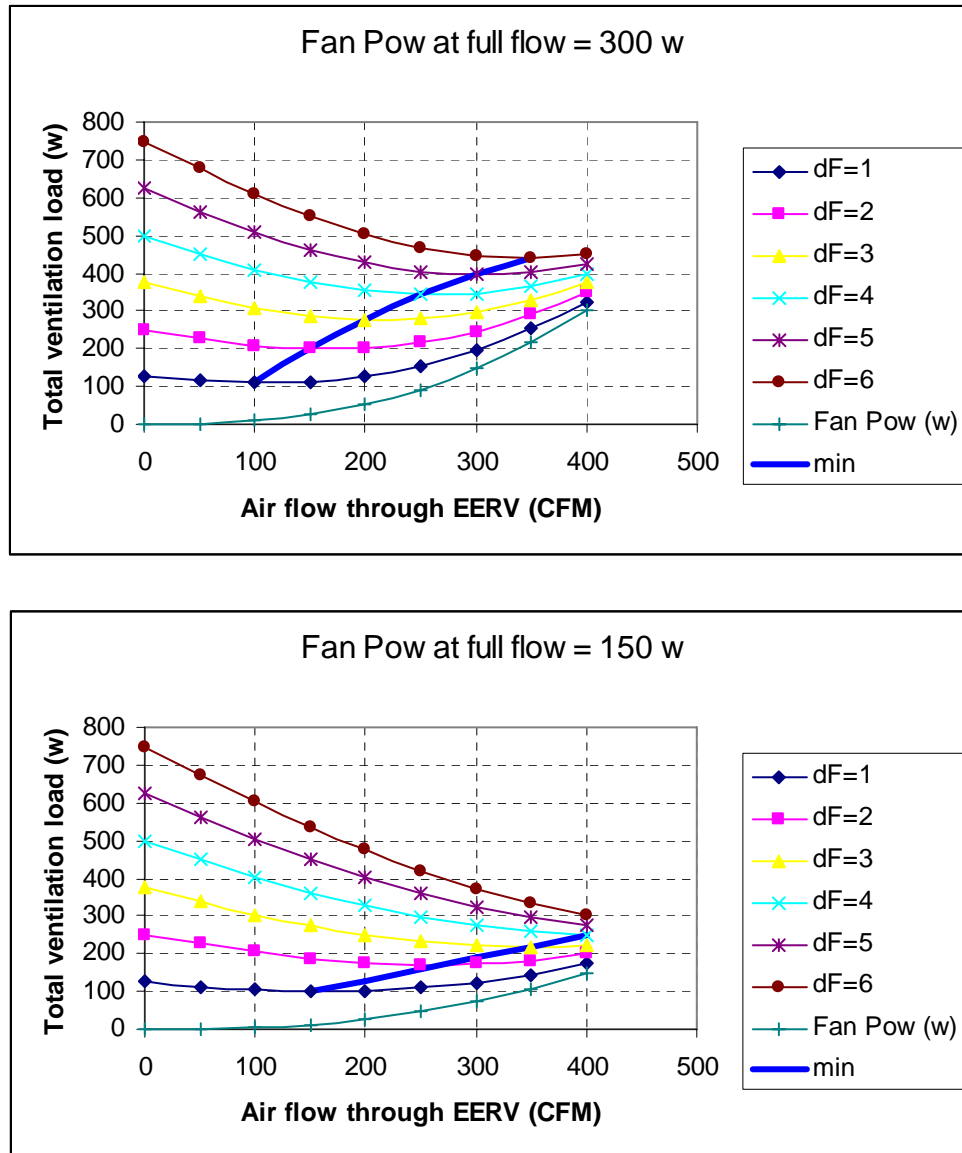


Figure 7.24. Total enthalpy load and fan power shown for a) 300 W fan power at 400 cfm, and b) 150 W fan power at 400 cfm.

In our experiment the fan power was approximately 150 W. In this example the band where partial fan speed is desirable is about 4 degrees differential F.

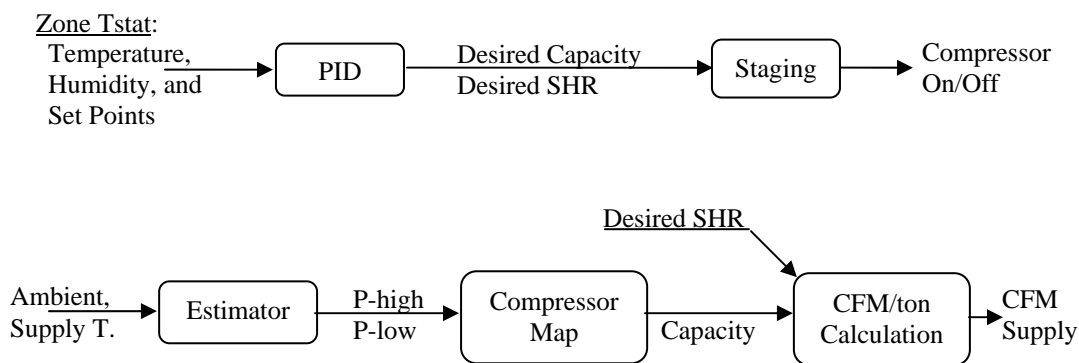
Control of the Exhaust Fan

In order for recovery to be successful, the exhaust air flow rate must be close in magnitude to the fresh air flow rate. This produces a balanced flow condition in the EERV recuperator. In most buildings it is desirable to keep the occupied space at a slightly elevated pressure relative to ambient. This is done by providing more supply air flow than return air flow. If there were no leaks in the rooftop and ducts then this would require that the exhaust fan provide a lower scfm than the boost fan through the core. However, the mixing plenum region of the rooftop unit is below atmospheric pressure and leaks from the outside into the mixing plenum will result in the supply air (equal to leaks plus return air) being higher the return and will serve the purpose of

pressurize the building. Therefore, it is recommended that the exhaust fan be controlled to match the exhaust scfm to the fresh.

Control of the Supply Fan

While the compressor is running, the supply fan speed should be varied to maintain the desired SHR over the coil. Increasing the air flow rate increases the SHR (reduces latent capacity). The advanced rooftop with integrated EERV should be designed to control both the zone humidity and temperature. For most applications an EERV will reduce the sensible and latent building loads, with a more significant reduction in latent. With the reduced loads the compressor size may be reduced. Since the latent load is reduced by a greater percentage than the sensible, the building SHR will increase. Therefore, the average building cfm/ton should also increase.



When the compressor is off, fan energy can be saved if the rooftop unit switches to 100% outside air. There are several ways that this can be accomplished.

1. Simply reduce the supply fan speed so that its cfm matches, or is slightly higher than, the fresh-air cfm. With this method fresh air from the EERV still passes over the wet coil when it is off. Water is re-evaporated, although not as quickly as it would be with full flow.
2. Bypass the fresh air from the boost fan around the coil directly into the supply duct. Either use automatic dampers, or run the supply fan very slowly to prevent backwards recirculation. With this method fresh air can be supplied with minimal re-evaporation from the coil.

Data Analysis

Two Excel “templates” have been devised for processing data taken in the system. The first allows rapid visual inspection of temperatures, relative humidity, humidity ratios, pressures and flows at many points in the system over the full run, to be able to assess the most appropriate sections of data to be further examined, depending on whether or not steady state or transient conditions are of interest. The second template does the automatic processing of the selected data. Despite the uncertainty in some of the data obtained and the difficulties being experienced in producing data of archival quality, the overall conclusion is that the energy recovered by the EERV appears comparable to that which was obtained in BP2.

Experimental issues

A difficulty encountered during an early run resulted in the accidental test of the core integrity when exposed to excess humidity and liquid water. During one of the initial test runs of the new integrated EERV system, the humidifier was mistakenly set at too high a generation rate. Excess humidity filled the ducts and rooftop unit. When this cooled on entering the EERV enclosure standing water was produced within the core box on each side (inlet and outlet) of the core. Apparently water had condensed within or near the core and poured out to the outlet side. After this water had evaporated, a residue remained on the outlet side of the core, especially on the exhaust stream side. There was a concern that this might have damaged the core by weakening the glue or distorting the membrane material. The membrane material used in the core is cross linked and is expected to be much more immune to water damage than predecessor materials that were not cross linked, even though best practice is to never permit condensation to appear. Therefore, new pressure drop measurements were taken for comparison with earlier work. The core pressure drop as a function of flow was found to not have been affected by this event.

Leaks in real systems

It was the desire of BP3 to use real hardware in an arrangement that could resemble a final product (although Plexiglas was used instead of sheet metal so that the core could be viewed, and flex ducts were used instead of direct connections so that modifications to flow paths could be easily made). Because of this there were several limitations in obtaining laboratory quality mass and energy balances.

- There was no way to measure the flow in the exhaust stream directly. The exhaust blower was mounted on the end of the core assembly and blew directly into the condenser chamber. There was not room to place a temporary duct and flow hood over this arrangement. The exhaust flow had to be calculated from the other known flows.
- A real economizer leaks when it is closed. Therefore, all of the fresh air drawn into the rooftop cannot be recovered. Additional leak paths also exist into the mixing plenum through the hinged doors and other sheet metal connections. If we had sealed up the economizer with tape and putty, then it would not be representative of a real system.
- Cores leak. A standard core is considered okay if the leak rate is less than 5%. Since we are using draw through fans the lowest pressures are in plenums (2) and (4) (see Figure 7.25). Leaks tend to occur from (1) to (4) and (3) to (2).

Analysis with System leakage

Analysis of the test data acquired during BP3 was made difficult due to system leakage. There are 3 major leak sources that were identified.

1. From the fresh air duct through the “closed” economizer to the mixing plenum.
2. From the condenser room through the rooftop panels into the mixing plenum.
3. Bypassing the core; both from (1) to (4) and from (3) to (2).

The Excel worksheet that had been developed for analyzing the integrated EERV/rooftop performance was modified to include the effects of leakage.

Note that in this section the 4 plenums around the core are referred to by the ARI-1060 test standard designations:

- 1) Fresh air in.
- 2) Fresh air out
- 3) Exhaust air (from return) in
- 4) Exhaust air out.

Each of these paths is shown in Figure 7.25. In a real unit (as opposed to our test facility) the first and second paths listed above would both leak “fresh” air into the mixing plenum, and can be treated as a single leak. In our test facility the condenser room’s humidity was not controlled as the “fresh” air was provided to the unit by mixing air from the humidity and the plenum chambers. Any leakage of fresh air into the mixing chamber, bypassing the EERV core, either increases the amount of fresh air or reduces the effective recovery.

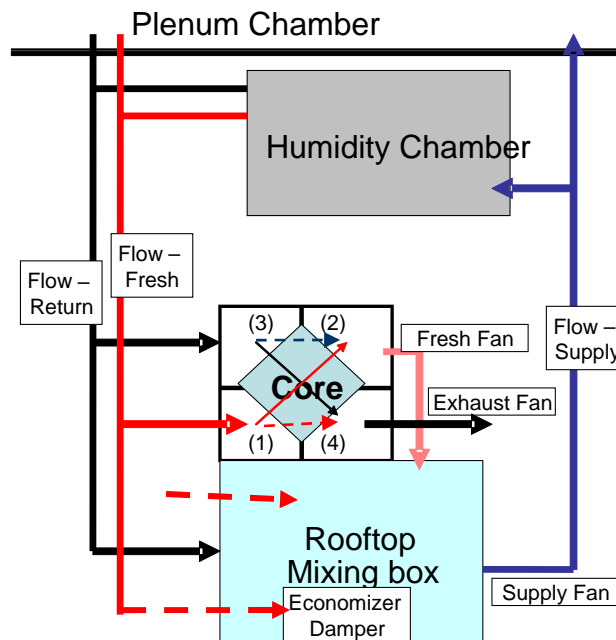


Figure 7.25. Experimental set up with leak paths shown.

Cross-core leaks are even more damaging to real recovery. What is counted as fresh air may in fact be recirculated stale air from the building. An example of how cross-core leaks affect the analysis is presented below.

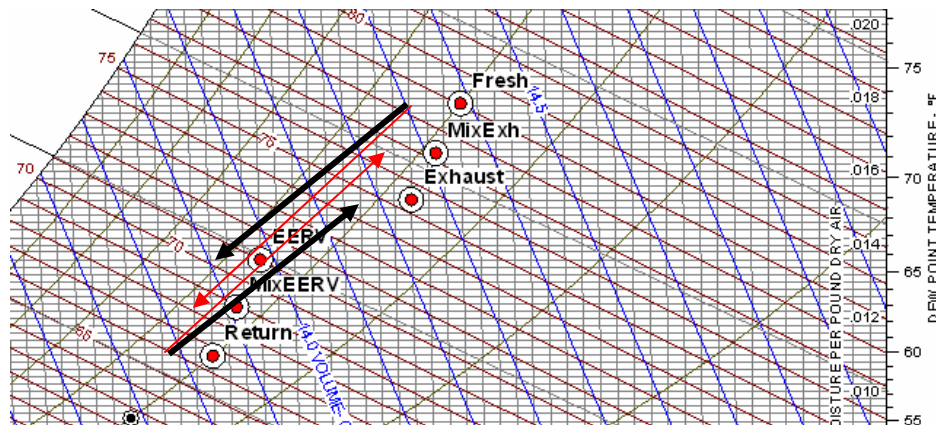


Figure 7.26. 50% mixing after recovery.

In this example the flows are balanced. The actual core effectiveness are:

Enthalpy effectiveness = 68%

Latent effective = 62%

If there is 50% mixing of recovered air with bypassed air for each stream (Fig. 7.26), the apparent effectiveness are higher:

Apparent enthalpy effectiveness = 84%

Apparent latent effective = 81%

Since the actual flow through the core would be only 50%, the effectiveness at full flow would be reduced according to the standard NTU-eff relations to:

Core enthalpy effectiveness at twice flow = 61%

Therefore, the apparent effectiveness of 84% would actually relate to a core that could provide only 61% at the proper flow rates.

If 50% of the “fresh” air is actually recirculated air, then the benefit of the EERV also needs to be reduced:

Actual recovery: $0.5 \cdot 68\% + 0.5 \cdot 0\% = 34\%$.

Experimental estimation of system leakage rates

A series of experiments were done to estimate the leakage rate of the core and economizer. To estimate the economizer leak, the supply fan was run at its normal speed but the fresh air fan was turned off, the economizer closed to 0%, and a tight sealing damper in the fresh air branch leading to the core was closed. With the mixing plenum at -0.3 inches of water about 100 CFM was measured in the fresh air duct.

As mentioned previously, the core was potentially damaged during the initial BP3 runs when the humidifier was turned on too high, and condensation flooded the ducts and core assembly. It is expected that the cross-linked membrane used in this core would be undamaged, but it is possible that the loosening glue or structures could result in leakage at the membrane edges (Fig. 7.27).

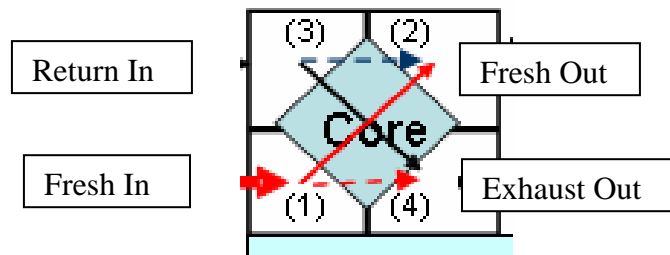


Figure 7.27. Schematic of just core assembly showing leakage paths.

A series of four CO₂ tests were performed:

1. Before Plugging leaks / Each fan driven with 4 Volts
2. Before plugging leaks / Exhaust fan increased to 5.5 Volts
3. After box was opened from the ends and tape was applied along boundaries, and modeling clay stuck into cracks. / Each fan at 4 Volts.
4. After box was sealed / Exhaust fan increased to 5.5 Volts.

For each of the tests

- The fans were run continuously.
- The return plenum was open to the condenser room, not connected to the return air duct. This helps to keep the pressure in the two inlet chambers better matched.
- Before starting the test the CO₂ level was measured in the room. Between tests the level was allowed to decay back to lower levels.
- To speed the response a suction pump was used to draw air samples into the CO₂ sensor cell.
- At time = 0, CO₂ was injected at a rate of about 20 SLPM into quadrant (or plenum) (1) [the fresh air intake].
- For the first 1 to 2 minutes CO₂ was sampled in quadrant (2) [fresh air exit].
- After this time the CO₂ sensor was moved to quadrant (4) [Exhaust air exit]. Ideally this plenum would track at no higher than the background level. The level was first measured at the plenum exit, just upstream of the exhaust fan. The level was then moved to explore the cavity, mostly on the bottom-middle region.
- CO₂ levels were re-checked in the room and other plenums before turning off the supply and completing the test.

Data from tests 3 and 4 are presented below (Fig. 7.28-7.30).

Leakage tests conclusions:

- The concentration at the exit of plenum (4) was almost as high as the concentration at the exit of plenum (2).
- The greatest concentration in either of plenums (2) or (4) was found at the bottom edge of plenum (4).
- It appears that air flows just as easily from (1) to (4) as from (1) to (2).
- The core has failed in that it does not keep the two air streams separate.

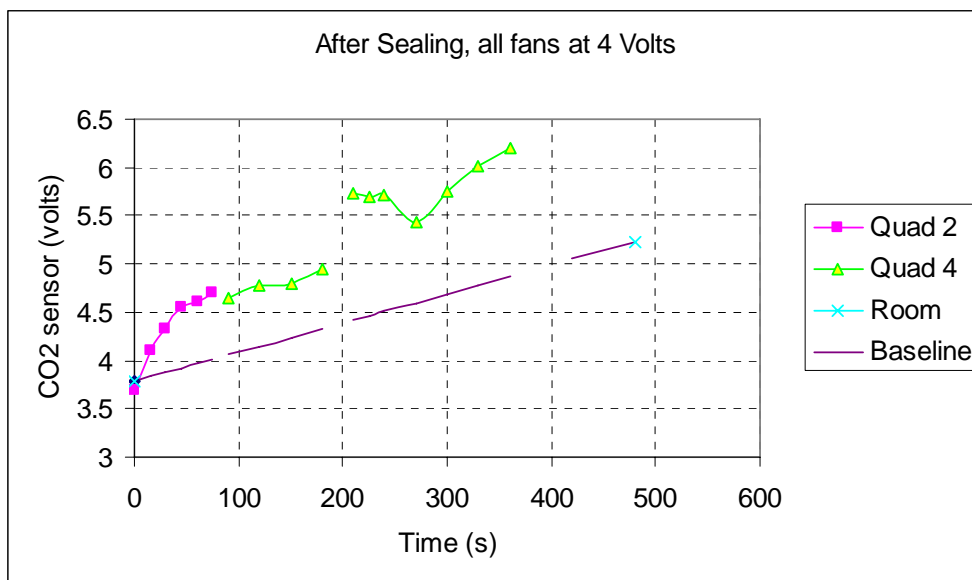


Figure 7.28. Third in a series of CO₂ leak tests. This test was done after the box was opened and potential leak paths within the box itself were sealed with clay and metallic tape. At time zero CO₂ was flowed into plenum (1), and measurements began in plenum (2). At 90 seconds into the test the CO₂ probe was moved to plenum (4).

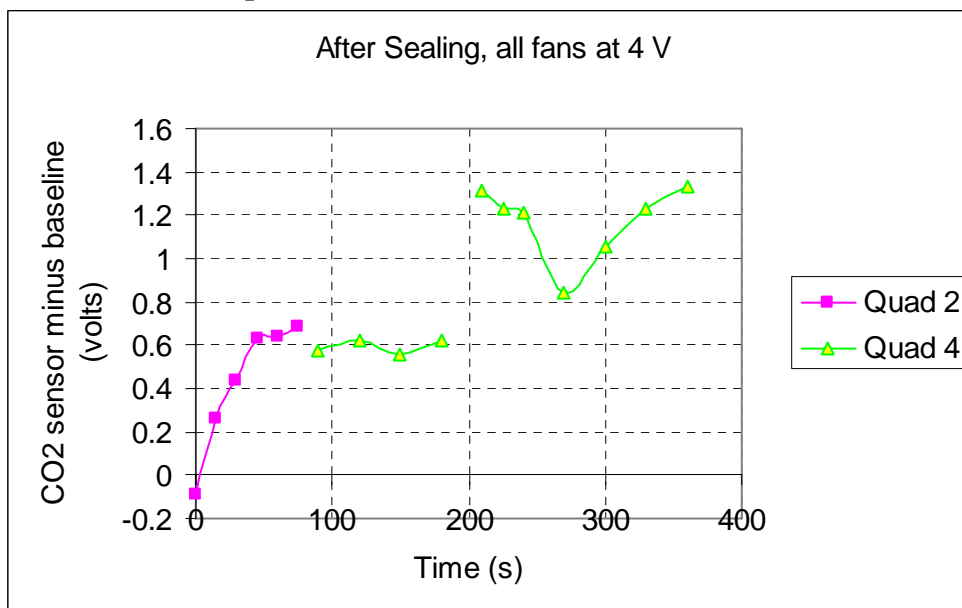


Figure 7.29. Same run as Figure 7.28 above, but the baseline voltage has been subtracted from each of the two lines to remove the effect of the rising background.

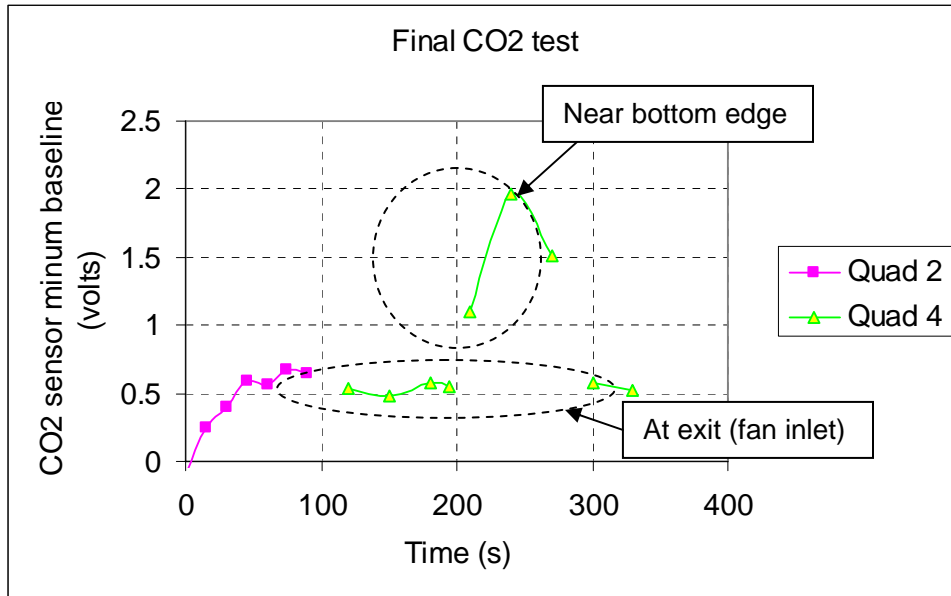


Figure 7.30. Final CO₂ leak test. Same condition as previous test except that the exhaust fan was run at a higher speed.

Other evidence for excessive core leakage

- Changing the exhaust fan speed changes the fresh air flow rate.
- Blocking the return air inlet and running the exhaust fan produces flow out of the exhaust fan and in to each of the fresh air openings. Ideally there would be no flow in this case.
- Blocking the fresh air inlet and running the fresh air boost fan produces flow out of the fresh air fan and in through the exhaust air openings.

It was also decided that a physical inspection of the core was needed. This was arrived at from the results of the CO₂ flow tracking after sealing any obvious leaks in the ducting and box. The response times for CO₂ getting from one side of the core to the other indicated the possibility of some convective flow due to small cross plate pressure differences. Physical inspection indicated some areas of debonding of the edge of the membrane plate to the closure bar. In addition, an analysis was carried out of the residue observed after the high humidity incident. Its melting point is 127 °C and decomposes at slightly higher temperatures. When dissolved in water it generates an acid solution. The analysis suggests it is a natural product

If resources become available for further technical work, it will be advisable to replace the core. This would permit the existing core to be studied more closely.

8.0 Results and Discussion

The following chapters summarize the analysis and interpretation of the data obtained in the experimental program. Section 8.1 gives an overview of some of the reliability analysis needed to sustain product development gate reviews. Chapter 9.0 discusses commercialization readiness and remaining needed steps. Conclusions and Recommendations are in Chapter 10.0.

8.1 EERV Reliability Analysis

The lifetime and reliability of the EERV system in the end application will have a large impact on its viability as a product. This fact drove the need for establishing quantifiable life and reliability goals and analyzing the EERV system versus these goals. This reliability analyses included:

1. Modeling and predicting the EERV system reliability.
2. Identifying major failure modes, their causes, their likelihoods and the severity of their effects.
3. Defining steps to reduce the likelihood of the identified failure modes and severity of their potential effects.
4. Defining steps to improve the fidelity of the reliability prediction and methods for improving the overall reliability.

Life and Reliability Requirements

A preliminary set of EERV system life and reliability requirements were established in order to provide a meaningful goal against which to measure the reliability predictions. These requirements are listed in the table below.

Table 8.1 EERV Reliability Requirements

Description	value	units
Failure Rate	$< 1.8\text{E-}6$	hrs ⁻¹
First Year Field Failure Rate (FFR1)	$< 1.5\%$	
Core Life	5	years
EERV Balance of Plant Life	15	years

In addition, a secondary requirement of reliability at five years was extrapolated from the primary requirements above. This secondary requirement is for a five year cumulative failure rate of $< 8\%$. These reliability requirements were used to guide the analysis and reliability improvement plans below.

Reliability Modeling and Prediction

A reliability prediction was conducted for the EERV system and compared to a similar prediction for an enthalpy wheel system. These predictions were then compared to the established reliability requirements. The core reliability was estimated for this model assuming a mature technology core with no significant wear-out modes in the required five-year life. Based on this assumption, a constant failure rate model was selected for this prediction. This model has a exponential probability distribution $f(t)$ of the form:

$$f(t) = \lambda e^{-\lambda t}$$

where λ is the failure rate in units of hour⁻¹ and t is the time in hours. The cumulative failure probability, $F(t)$ is then given by:

$$F(t) = 1 - e^{-\lambda t}$$

And the reliability $R(t)$ is given by:

$$R(t) = e^{-\lambda t}$$

This model allows for addition of failure rates for the various failure modes based on the formula:

$$\lambda_T = \sum_{i=1}^N \lambda_i$$

Where λ_i is the constant failure rate associated with failure mode i and λ_T is the total failure rate of the system.

Besides the core, other data input to the EERV reliability model were from component field data for components similar to those that will be needed in an EERV system. These other components include a blower, damper, damper actuator and wiring. This prediction was compared to a similar assessment of an enthalpy wheel system. This early assessment showed that the EERV with a mature core had a superior predicted typical reliability at 5 years of 93% to that predicted for an enthalpy wheel system, 72%.

It was concluded that future reliability assessment and assurance work should include improving the fidelity of the estimates for the component reliability data feeding the model as well as analytical and experimental work to validate the membrane and core reliability.

A close comparison of the Failure Modes and Effects Analyses (FMEA's) and reliability prediction spreadsheets for the plate EERV and the enthalpy wheel showed some mismatch in system configuration assumptions. For instance, a heater to prevent frost that was present in the wheel configuration was added to the membrane EERV system description. When these assumptions were fully harmonized, the effect on the reliability predictions was small. Specifically, the updated reliability predictions showed that the expected value of reliability at five years for the EERV had changed slightly from 93% to 92%, while the expected value for reliability of the enthalpy wheel had improved from 72% to 86%.

One source of the change in the value for the EERV was that the assumption for failure rate for the mature EERV membranes compared to the wheel active element was changed from parity to the EERV membranes having a 50% higher failure rate than the wheel active element. This change was based on the reasoning that the more complex chemistry of the EERV membranes, even when mature, might still be somewhat more susceptible to unusual spikes in certain contaminants than the simpler chemistry of the desiccant wheel. Even with these changes, the membrane EERV system still has a predicted reliability better than that of the enthalpy wheel system.

Risk Identification and Assessment

A failure mode and effects analysis (FMEA) was conducted on both the EERV and an enthalpy wheel system with equivalent component list to accomplish similar functions to EERV. Failure modes get ranked on likelihood of occurrence, whether they will be detected before reaching the end user and the severity of impact. The severity scale ranges from effects that result in only nuisance faults to items that result in loss of primary system function to ones that may result in a safety or environmental hazard.

Highest identified risks for the enthalpy wheel included:

- Air seal partition wear
- Wheel drive belt slippage / failure
- Failure of heater for frost control
- Wheel failure due to condensation cycling, moisture barrier and other stressors
- Wheel bearing failure

Highest risks for the enthalpy plate EERV included:

- Membrane failure due to aging, chemical attack, moisture barrier formation
- Adhesive failure due to aging or chemical attack.

The adhesive failure is easily mitigated by adhesive selection or elimination from the design.

Other common failure risks for both systems included:

- Fan failure
- Damper actuator failure
- Filter failure due to improper maintenance

From a review of these potential failure risks, it can be seen that if the robustness of the membranes themselves are proven, the remainder of the plate system has fewer reliability risks than the wheel system.

Risk Mitigation Planning

After identifying the risks and ranking them, the standard (UTRC proprietary) product development process requires that a risk reduction plan be formulated. Major identified risks included membrane reliability relative to chemical contaminants and core reliability relative to frost, adhesive and dust.

The detailed FMEA spreadsheet also includes many additional detailed risk mitigations targeted at the individual identified risks. In addition, a detailed plan for quantifying the membrane reliability was developed.

Detailed membrane reliability test plan outline

Since the membranes have the greatest uncertainty in the risk level due the lack of full knowledge of the possible chemical interactions and degradation mechanisms over time, an outline of a test plan was prepared that would guide reliability assessment and improvement efforts for the membrane core. The purpose of this test plan outline is to define desired tests of the enthalpy exchange membranes to better assess their reliability. The results from these tests will enable the estimation of model parameters that relate the

membrane performance and life to the stress level and time in the end use environment for identified critical stressors. These critical stressor models can then be used to perform a more valid prediction of reliability versus time in the field and can be used to refine replacement and possible maintenance strategies as well as to assess the financial risks of adopting this new technology.

Membrane Test Plan Overview

This test plan outline describes the process needed to identify the most critical stressors of the enthalpy membranes and to produce models that will allow estimation of reliability of the enthalpy cores versus time in the end-use environment. The steps in this process include the following:

1. Comprehensive identification of likely membrane stressors in end use environment
2. Initial narrowing of this list to more critical stressors
3. Phase I testing to identify the small number of most critical stressors
4. Phase II testing to produce data to allow extraction of degradation model parameters for each of these stressors

Stressor Identification, Narrowing and Phase I Testing

A literature review and expert panel can be used to identify possible chemical stressors and their relative possible impacts on the membranes. The stressors with risk levels above a chosen threshold would be used in the Phase I testing to further identify the most dominant stressors and stressor interactions. Phase 1 testing would consist of a two-level half-factorial experimental design to limit the number of test runs and whose output would be a very small list of primary stressors and interactions. This shortened list of critical stressors would be the input for the Phase II testing.

Phase II Testing

In Phase II Testing, additional tests will be performed to quantify the relation between exposure to the stressors and the membrane performance in terms of moisture transfer. If these remaining critical stressors were shown to be independent – not included in a secondary effect with another factor, these stresses can be analyzed individually using a life stress model. First, a life model must be chosen to relate the failure probability of membranes exposed to a given stressor. The two-parameter Weibull model is generally a good choice for a life model as it fits many types of failure distributions. The equation of the two-parameter Weibull probability density function is shown below.

$$f(t) = \frac{\beta}{\eta} \left(\frac{t}{\eta} \right)^{\beta-1} e^{-\left(\frac{t}{\eta} \right)^{\beta}}$$

where:

f is the failure probability density as a function of time

t is time

β is the shape factor

η is the characteristic life

Next, a model must be chosen relating the stress level to the life characteristic. Since the membrane manufacturer may know some of these relations, they should endeavor to do this selection. The Arrhenius life versus stress model is often appropriate. The Arrhenius model is given by:

$$L(V) = C \bullet e^{\frac{B}{V}}$$

where:

L is a quantifiable life measure

V is the stress level

C is one model parameter

B is the other model parameter

This Weibull life model and Arrhenius acceleration model can be combined to yield a single model that could be fitted from an appropriate data set. The process of fitting data to the Weibull / Arrhenius model assumes that the effects from the main stressors / factors are independent. A more complex life/acceleration model combination would need to be chosen for any stressors that demonstrated two factor interactions.

Model Building and Reliability Prediction

The Phase II test data will be analyzed to extract the model coefficients. This can be done conveniently with available commercial software packages such as ReliaSoft. Once the life model parameters for each stressor have been extracted these models can be combined into a more comprehensive single reliability model where the inputs are the expected range of environmental conditions for each critical stressor. This reliability model can then be used to yield a prediction of expected reliability versus time and cumulative failure probability at end of the design life (5 years). This can be done with ReliaSoft, Sigma Plot, Crystal Ball or Minitab software packages. This more valid prediction of reliability versus time in the field can then be used to refine replacement and possible maintenance strategies as well as to better quantify the risks versus benefits of adopting this new technology.

9.0 Commercialization Plan

This Cooperative Agreement is aligned with the UTC/Carrier product development/commercialization process. While the ordering of steps is slightly different due to changes that have occurred in the process since this project was proposed, it has proceeded regularly through the process. Much of the work of Phase I of the Cooperative Agreement fell under UTC Gates 0 through 3. One exception was the modeling of specific applications that occurred in Phase II. The UTC gates align with Carrier “Passport” stage gates and UTC gates starting with Gate 3 require the direct participation of Carrier product development managers. This project has passed UTRC Gate 3 and Carrier Passport 0. This means that there is a formal project within Carrier that is examining the market opportunity and other elements of their process. The Carrier process considers a wider set of specific product preparation and launch questions are asked in the Carrier reviews including field demonstration requirements and results and projected reliability characteristics. Parallel work is conducted by UTC and Carrier to address the issues that arise in these reviews, some of which may fall outside the current scope of this project.

The technical work shows no significant performance showstoppers in deploying this energy recovery technology. However, as it matures and gets compared to enthalpy wheels, the area of highest concern continues to be the uncertainty surrounding the longevity of the membrane. It is conjectured that it is potentially susceptible to long-term degradation from air contaminants that may arise in either indoor or outdoor air. In buildings, spikes in volatile organic compounds can arise from cleaners as well as outgassing from building materials, especially during renovations. There can be spikes in ozone or other contaminants outdoors. More quantitative estimates of failure rates are needed for future evaluations of this technology in the product development process, as commercialization opportunities arise. UTRC supplied DOE with a plan developed from a formal risk analysis of all types of risk for technology deployment that would reduce this uncertainty in a timely manner. DOE responded that no resources were available for addressing this area of concern. The uncertainty that surrounds this issue arises in discussions of commercialization prospects.

10.0 Conclusions

The effectiveness factors of the EERV was measured to be 0.75 sensible, 0.70 latent. At the 30% outside air fraction condition used a “System EER” of about 15 was demonstrated—an increase in EER of about 25% over the EER of the HVAC unit. The concept of a System EER is part of new ARI Guidelines V and W.

The greatest technical hurdle in BP1 was meeting the stretch objective of nearly a factor of three in latent performance without sacrificing sensible effectiveness in the same volume and at nearly neutral projected cost. While the original approach using LBM if developed further might ultimately prove technically and economically successful, the current spacer design met the program goals cost effectively. The resultant latent effectiveness nearly matches the sensible effectiveness. While numbers closer to the theoretical limit of 1.0 can be reached by making much larger devices, the space and cost constraints would be prohibitive. BP2 and BP3 met their performance goals, demonstrating that this technology can perform adequately. From a manufacturer’s perspective this technology competes with the more mature enthalpy wheel approach. It is clear the most attractive size range is the smaller end (< 20 tons) where the wheels are relatively more expensive per cfm and the flat plate devices have the distinct advantage of low maintenance. The largest barrier to commercialization will be to get into production quantities that make the technology cost effective in its own right without government subsidies. The manufacturability study from BP1 is helpful in charting this path. A secondary concern is longevity. This program concentrated on demonstrating performance and benefits. Before this technology is commercialized resources must be found to conduct field studies that show that in the actual conditions of a building with the usual indoor and outdoor air contaminants that the EERV element substantially retains its performance properties over the five year warranty that is common in the industry, or that the cost of periodic replacements can be made low enough (as with filters).

1. Major Accomplishments:

BP1: Design of an optimized flat plate energy recovery ventilator with latent effectiveness about three time higher than those commercially available under similar conditions. Completion of Product Development Gate 2. Completion of a manufacturability study that shows this technology can be nearly cost neutral in production volumes.

BP2: Demonstration of a flat plate EERV unit integrated into a downsized unitary HVAC unit having a system EER about 25% higher than a conventionally sized unit without energy recovery. Demonstration of about one ton of energy recovery when operating at three tons of cooling capacity. Construction of a EnergyPlus/Matlab software system that can semi-automatically produce national maps of energy recovery viability and performance. Completion of Product Development Gate 3.

BP3: Demonstration of a refined design for integrating flat plate energy recovery devices with unitary equipment using variable speed fans. Completion of Product Development Gate 3.5.

2. Patent Disclosures:

R-05858: Method for Energy Recovery Ventilator Reliability Improvement and Life Extension

R-05856: Method for Seasonal Adjustment of Energy Recovery Ventilator Performance

R-05633: Flat Plate Heat Exchanger with Asymmetric Interplate Gap or Spacer Design

3. Publications:

Simulation of the effect of an energy recovery ventilator on indoor thermal condition and system performance, Proceedings of the Ninth International Building Performance Simulation Association Conference, Montreal, QC, August 15-18, 2005.

Recent Advancements in High Latent Recovery Effectiveness Membrane Flat Plate Heat Exchangers for Air-to-Air Energy Recovery from Ventilation Air, Seminar 44, ASHRAE Annual Meeting, Denver, CO, June 26-29, 2005.

IEQ and energy benefits with an enhanced energy recovery ventilator. F. J. Cogswell, J. A. Davies, G. M. Dobbs, and N. O. Lemcoff, 2004 Syracuse Symposium on Environmental and Energy Systems, Syracuse, NY, October 25-26, 2004

Cost Effective Indoor Air Quality. N. O. Lemcoff, G. M. Dobbs – Indoor air quality problems and engineering solutions Specialty Conference, EPA/AWMA, Research Triangle Park, NC, July 21-23, 2003.

11.0 Principal Project Personnel

Dr. Gregory M. Dobbs, Principal Scientist

United Technologies Research Center, 411 Silver Lane, East Hartford, CT 06108

Phone: 860-610-7145, Fax: 860-660-1092, e-mail: dobbsgm@utrc.utc.com

Dr. Norberto O. Lemcoff, Principal Engineer

United Technologies Research Center, 411 Silver Lane, East Hartford, CT 06108

Phone: 860-610-7024, Fax: 860-660-9962, e-mail: lemcofno@utrc.utc.com

Dr. Frederick J. Cogswell, Principal Engineer

United Technologies Research Center, 411 Silver Lane, East Hartford, CT 06108

Phone: 860-610-1688, Fax: 860-660-1068, e-mail: cogswefj@utrc.utc.com

Prof. Stephen R. Lee, AIA

Center for Building Performance and Diagnostics, Department of Architecture, Carnegie Mellon University, 5000 Forbes Avenue, Pittsburgh, PA 15213

Phone: 412-268-3528, Fax: 412-268-6129, e-mail: stevelee@cmu.edu

12.0 References

- Henderson, Hugh I., Jr. and K. Rengarajan (1996). A Model to Predict the Latent Capacity of Air Conditioners and Heat Pumps at Part-Load Conditions with Constant Fan Operation. ASHRAE Transactions. Paper No. 3958, Vol. 102, Part 1, pp. 266-274.
- Niu, J. L. and L. Z. Zhang (2001). Membrane-Based Energy Recovery Ventilators: A Solution to Heat Recovery for Ventilation Air in Hong Kong. Transactions of the Hong Kong Institute of Engineers, Vol. 8, No. 2, pp. 58-63.
- Niu, J. L. and L. Z. Zhang (2001). Membrane-based Enthalpy Exchanger: Material Considerations and Clarification of Moisture Resistance. J. Membrane Sci., Vol. 189, No. 2, 179-191.
- Niu, J. and L. Zhang (2002). Potential Energy Savings for Conditioning Fresh Air with a Membrane-Based Energy Recovery Ventilator. Paper No. 4497, ASHRAE Transactions, Vol 108, Pt. 1.
- TIAX (2002). Energy Consumption Characteristics of Commercial Building HVAC Systems Volume III: Energy Savings Potential Final Report, TIAX LLC, July, 2002.
- Zhang, L. Z. and Y. Jiang (1999). Heat and Mass Transfer in a Membrane-Based Energy Recovery Ventilator, J. Membrane. Sci., Vol. 163, pp. 29-38.
- Zhang, Y, Y. Jiang, L. Z. Zhang, Y. Deng, and Z. Jin (2000). Analysis of thermal performance and energy savings of membrane based heat recovery ventilator. Energy, Vol. 25, pp. 515-527.
- Zhang, L. Z. and J. L. Niu (2001). Energy requirements for conditioning fresh air and the long-term savings with a membrane-based energy recovery ventilator in Hong Kong. Energy, Vol. 26, 119-135
- Zhang, L. .Z. and J. L. Niu. (2002). Effectiveness Correlations for Heat and Moisture Transfer Processes in an Enthalpy Exchanger with Membrane Cores. Transactions of the ASME, Vol. 124, October, pp. 922-929.

13.0 List of Acronyms and Abbreviations

acfm	actual cubic feet per minute
ARI	Air Conditioning and Refrigeration Institute
ASHRAE	American Society of Heating, Refrigeration, and Air Conditioning Engineers
BP	budget period
btu	British Thermal Unit
CAT	Center for Automation Technology
CAV	constant air volume
CBPD	Center for Building Performance and Diagnostics
CCN	Carrier Comfort Network
cfm	cubic feet per minute
CMU	Carnegie Mellon University
DB	dry bulb
DC	direct current
DOE	Department of Energy
DX	direct expansion
ECM	electronically commutated motor
ERV	energy recovery ventilator
FFR	field failure rate
FMEA	failure modes and effects analysis
HVAC	heating, ventilation and air conditioning
EERV	enhanced energy recovery ventilator
HRV	heat recovery ventilator
LBM	lattice block material
lpm	liters per minute
lps	liters per second
NETL	National Energy Technology Laboratory
NREL	National Renewable Energy Laboratory
psi	pounds per square inch
RH	relative humidity
RPI	Rensselaer Polytechnic Institute
scfm	standard cubic feet per minute
slpm	standard liters per minute
SHR	sensible heat ratio
TMY	Typical Meteorological Engineer
TR	tons of refrigeration
UTC	United Technologies Corporation
UTRC	United Technologies Research Center
VAV	variable air volume
WB	wet bulb
w.c.	water column